Lawrence Livermore National Laboratory

Supplemental Material S1 to S3

for

The Regional Relative Risk Metric

Michael B Dillon
Charles F Dillon

August 2020

LLNL-JRNL-814116

Lawrence Livermore National Laboratory is operated by Lawrence Livermore National Security, LLC, for the U.S. Department of Energy, National Nuclear Security Administration under Contract DE-AC52-07NA27344.

Auspices and Disclaimer

Lawrence Livermore National Laboratory is operated by Lawrence Livermore National Security, LLC, for the U.S. Department of Energy, National Nuclear Security Administration under Contract DE-AC52-07NA27344.

Financial support was provided, in part, by the US Department of Homeland Security for related early efforts. Research was supported, in part, by the DOE Office of Science through the National Virtual Biotechnology Laboratory, a consortium of DOE national laboratories focused on response to COVID-19, with funding provided by the Coronavirus CARES Act.

Description of Supplemental Files

Supplemental Material S1: General Theory

This supplemental material derives key theoretical concepts and equations that are implemented in the main paper.

Supplemental Material S2: Outdoor Normalized Time and Space Integrated Air Concentrations

This supplemental material describes how outdoor exposures were calculated and provides downwind exposure estimates, as well as absolute and relative infection probabilities, for a wide range of meteorological conditions and airborne loss rates.

Supplemental Material S3: Key Atmospheric Transport and Dispersion Modeling Concepts

This supplemental material provides information on key atmospheric physics and meteorological concepts, dispersion models (including accuracy and validation), and the theoretical rationale for using the space and time integrated air concentration metric.

Supplemental Dataset D1: Outbreak Model-Measurement Comparison

This spreadsheet documents the disease outbreak data and analysis methods used to calculate results presented in the main document, where model predictions are compared to actual disease outbreak data.

Supplemental Material S1: General Theory

Michael B Dillon

In this supplemental material, we derive key theoretical concepts that are implemented in the main paper. Theoretically, the total number of infections can be calculated by individually considering every exposed person. However, this approach can be challenging to implement due to computational considerations, including the need to acquire high resolution input data, which is often not available. Also such approaches potentially obscure useful interpretations. Therefore to facilitate the use of **Equations 1, 2,** and **3** presented in the main paper, we derive here a series of self-consistent equations for exposure and infection probability applicable to individuals (indicated by the index *p*), (sub)groups of individuals with the same exposure but varying individual response to exposure (index *s*), groups of individuals with varying individual exposures and individual responses to a given exposure (index *g*), and geographic regions containing a specified group of people (index *r*).

S1 Variable Definitions

r = a specific geographic region

r_{ref} = a geographic region used as a reference in a relative incidence analysis

r_{source} = a geographic region where infectious airborne particles are emitted

p = an individual person that could be infected, i.e., a susceptible individual

TP = total number of exposed, susceptible individuals

s = a specific (sub)group of individuals with the same exposure but varying responses to that exposure

TS = total number individuals in (sub)group *s*

g = a specific group of individuals with varying exposures and responses to the given exposure

TSG = total number of subgroups in group *g*

particle type = specifies particle size and infectivity as a function of time and environmental properties

b = a specific particle type

TB = total number of particle types

$[Adjustment\ Factor](g,b)$ = scaling factor for group *g* that accounts for the deviation of *b*-type particle exposure and response from that of the reference exposure and response (no units)

$[Adjustment\ Factor](r,b)$ = scaling factor for region *r* that accounts for the deviation of *b*-type particle exposure and response from that of the reference exposure and response (no units)

$[Area](r)$ = area of region *r* (m^2)

$[Effective\ Source\ Term](r, r_{source}, b)$ = mathematical construct used to scale infection probability from one region to another for *b*-type particles. ($m^3\ s^{-1}$ people^{-1})

$[Exposure](p)$ = number and type of infectious airborne particles in the breathing volume (respiratory second volume)[1] of individual *p* (particles s m^{-3})

$[Exposure](p,b)$ = the number of *b*-type infectious airborne particles in the breathing volume (respiratory second volume) of individual *p* (particles s m^{-3})

$[Exposure](s,b)$ = number of *b*-type infectious airborne particles in each individual's breathing volume (respiratory second volume) for individuals in (sub)group *s* (particles s m^{-3})

$[Exposure]_{ref}(g,b)$ = reference number of *b*-type airborne particles in the breathing volume (respiratory second volume) of an individual in group *g* (particles s m^{-3})

$[Exposure]_{ref}(r,b)$ = reference number of *b*-type airborne particles in the breathing volume (respiratory second volume) of an individual in region *r* (particles s m^{-3})

$[Exposure\ Adjustment\ Factor](g,s,b)$ = scaling factor that for group *g*, subgroup *s* accounts for the deviation of *b*-type particle exposure from the reference exposure (no units)

$[Exposure\ Adjustment\ Factor](r,s,b)$ = scaling factor that for region *r*, subgroup *s* accounts for the deviation of *b*-type particle exposure from the reference exposure (no units)

$Health\ Effect\ Model\big(p,[Exposure](p)\big)$ = mathematical model describing the probability that an individual *p* will be infected given the individual's specific exposure (no units)

[1] Respiratory minute volume is a traditional unit in pulmonary medicine – this study uses respiratory second volume.

$[Infection\ Probability](p)$ = probability that an individual *p* becomes infected (no units)

$[Infection\ Probability](p, b)$ = probability that an individual *p* becomes infected by becomes infected by a *b*-type particle (no units)

$[Infection\ Probability](s)$ = mean probability that a random individual in (sub)group *s* becomes infected. All individuals in (sub)group *s* have the same exposure. (no units)

$[Infection\ Probability](g)$ = mean probability that a random individual in group *g* becomes infected (no units)

$[Infection\ Probability](r)$ = mean probability that a random individual in region *r* becomes infected (no units)

$[Infection\ Probability](r, b)$ = mean probability that a random individual in region *r* becomes infected by a *b*-type particle (no units)

$[Infections]$ = total number of people infected (people)

$[Infections](r, b)$ = total number of people infected by *b*-type particles in region *r* (people)

$[Infectious\ People](r_{source})$ = total number of people capable of emitting infectious particles in source region r_{source} (people)

$[Metric\ of\ Interest\ Probability](p)$ = probability that an individual *p* exhibits the metric of interest (no units)

$[Normalized\ TSIAC](r, b)$ = *b*-type particle air concentration integrated over region *r* and the passage of an airborne infectious plume assuming a single particle was released at the source (s m^{-1})

$[Normalized\ TSIAC](r, r_{source}, b)$ = *b*-type particle air concentration integrated over region *r* and the passage of an airborne infectious plume assuming a single particle was released from source region r_{source} (s m^{-1})

$[Population\ Density](r)$ = population density in region *r* (people m^{-2})

$[Population\ Probability](g, s)$ = probability that an individual in group *g* is in subgroup *s* (no units)

$[Relative\ Infection\ Probability](r, b)$ = ratio of the region *r* infection probability to reference region infection probability due to exposure to *b*-type particles (no units)

$[Release\ Probability](b)$ = probability that a particle released into the environment is a *b*-type particle (no units)

$[Response\ Adjustment\ Factor](g, s, b)$ = scaling factor that for group *g*, subgroup *s* accounts for the deviation of *b*-type particle response from the reference response (no units)

$[Single\ Particle\ Infection\ Probability](p, b) =$ the probability that individual *p* will become infected after being exposed to a single *b*-type particle. This term includes, but is not limited to, the probability that particle(s) will be inhaled and deposit in the respiratory system. ($m^3\ s^{-1}$ $particle^{-1}$)

$[Single\ Particle\ Infection\ Probability](s, b)$ = the mean probability that a random individual in (sub)group *s* will become infected after being exposed to a single *b*-type particle. This term includes the probability that particle(s) will be inhaled and deposit in the respiratory system. ($m^3\ s^{-1}$ $particle^{-1}$)

$[Single\ Particle\ Infection\ Probability]_{ref}(g, b)$ = reference probability that an individual in group *g* will become infected after being exposed to a single *b*-type particle. This term includes the probability that particle(s) will be inhaled and deposit in the respiratory system. ($m^3\ s^{-1}$ $particle^{-1}$)

$[Single\ Particle\ Infection\ Probability]_{ref}(r, b)$ = reference probability that an individual in region *r* will become infected after being exposed to a single *b*-type particle. This term includes the probability that particle(s) will be inhaled and deposit in the respiratory system. ($m^3\ s^{-1}$ $particle^{-1}$)

$[Single\ Particle\ Metric\ of\ Interest\ Probability](p, b) =$ the probability that individual *p* will exhibit the metric of interest after being exposed to a single *b*-type particle. This term includes the probability that particle(s) will be inhaled and deposit in the respiratory system. ($m^3\ s^{-1}$ $particle^{-1}$)

$[Source\ Adjustment\ Factor](r_{source}, b)$ = scaling factor that accounts for the deviation of *b*-type particles emitted from the r_{source} region from that of a reference source region (no units)

$[Subgroup\ Adjustment\ Factor](g, s, b)$ = scaling factor that accounts for the deviation of group *g*, subgroup *s*, *b*-type particle exposure and response from that of the reference exposure and response (no units)

$[Total\ Particles\ Released]$ = total number of particles released into the atmosphere (particles)

S1.1. Conceptual Model

The general environmentally-mediated infection process can be mathematically represented by **Equations A1** and **A2**.

(Equation A1)

$$[Infections] = \sum_{p=1}^{TP} [Infection\ Probability](p)$$

(Equation A2)

$$[Infection\ Probability](p) = Health\ Effect\ Model\big(p, [Exposure](p)\big)$$

S1.2. Rare Infections

For any individual (p) who is exposed to a collection of identical (b type) infectious particles, we assume that (i) they either become infected or not, (ii) the probability of becoming infected by a given particle is small, and (iii) the probability of becoming infected by two particles simultaneously is negligible. By the law of rare events, the infection probability is approximated by a Poisson distribution, with the expected value (mean) given by **Equation A3a**.

(Equation A3a)

$$[Infection\ Probability](p,b) \approx [Exposure](p,b) \cdot [Single\ Particle\ Infection\ Probability](p,b)$$

For the more general case in which an individual is exposed to a collection of different types of infectious particles, the infection probability can be approximated by the sum of independent Poisson distributions (one for each particle type), with the expected value (mean) given by **Equation A3b**.

(Equation A3b)

$$[Infection\ Probability](p) \approx \sum_{b=1}^{TB} \big([Exposure](p,b) \cdot [Single\ Particle\ Infection\ Probability](p,b)\big)$$

We note that an infectious particle can contain more than one pathogenic microorganism and be physically larger than the pathogen itself. Furthermore, *the pathogen dose-response function that determines the value of [Single Particle Infection Probability](p,b) can take any mathematical form and can vary by individual*.

S1.3. Subgroups

Consider a (sub)group *s* comprised of *TS* individuals with same exposure, but varying response to that exposure,[2] then **Equations A4** and **A5** provides the mean infection probability for (sub)group *s*.

(Equation A4)

$$
\begin{aligned}
&[Infection\ Probability](s) \\
&\equiv \frac{\sum_{p=1}^{TS}[Infection\ Probability](p)}{TS} \\
&\approx \frac{\sum_{p=1}^{TS}\sum_{b=1}^{TB}\left([Exposure](p,b)\ \cdot\ [Single\ Particle\ Infection\ Probability](p,b)\right)}{TS} \\
&= \sum_{b=1}^{TB}\left([Exposure](s,b)\ \cdot\ \frac{\sum_{p=1}^{TS}[Single\ Particle\ Infection\ Probability](p,b)}{TS}\right) \\
&= \sum_{b=1}^{TB}\left([Exposure](s,b)\ \cdot\ [Single\ Particle\ Infection\ Probability](s,b)\right)
\end{aligned}
$$

(Equation A5)

$$
[Single\ Particle\ Infection\ Probability](s,b) \equiv \frac{\sum_{p=1}^{TS}[Single\ Particle\ Infection\ Probability](p,b)}{TS}
$$

S1.4. Groups

When exposures within a group of people are not constant,[3] each subgroup can be considered a separate, constant exposure group and the overall group's (mean) infection probability is equal to the population weighted average of the individual subgroup infection probabilities, see **Equation A6**.

(Equation A6)

$$
\begin{aligned}
[Infection\ Probability](g) &= \sum_{s=1}^{TSG}\left([Population\ Probability](g,s)\right. \\
&\quad \left.\cdot\ [Infection\ Probability](s)\right) \\
&\approx \sum_{b=1}^{TB}\sum_{s=1}^{TSG}\left(\begin{array}{c}[Population\ Probability](g,s) \\ \cdot\ [Single\ Particle\ Infection\ Probability](s,b) \\ \cdot\ [Exposure](s,b)\end{array}\right)
\end{aligned}
$$

[2] One example is a group of people in a room where the air is well mixed.
[3] One example is a neighborhood where people are in different buildings that provide varying degrees of protection from an outdoor plume of airborne infectious particles.

We assume that each particle acts independently. As a consequence, the individual exposures and health effects can be defined as a ratio to a reference exposure and response, respectively. While these ratios can take any value and vary by individual, the individual-specific value cannot change. With these assumptions, **Equation A6** can be re-written as **Equation A7** to **A11**.

(Equation A7)

$$[Infection\ Probability](g) = \sum_{b=1}^{TB} \begin{pmatrix} [Single\ Particle\ Infection\ Probability]_{ref}(g,b) \\ \cdot\ [Exposure]_{ref}(g,b) \\ \cdot\ [Adjustment\ Factor](g,b) \end{pmatrix}$$

(Equation A8)

$$[Adjustment\ Factor](g,b) = \sum_{s=1}^{TSG} \begin{pmatrix} [Population\ Probability](g,s) \\ \cdot\ [Subgroup\ Adjustment\ Factor](g,s,b) \end{pmatrix}$$

(Equation A9)

$$[Subgroup\ Adjustment\ Factor](g,s,b) = [Exposure\ Adjustment\ Factor](g,s,b) \cdot [Response\ Adjustment\ Factor](g,s,b)$$

(Equation A10)

$$[Exposure\ Adjustment\ Factor](g,s,b) = \frac{[Exposure](s,b)}{[Exposure]_{ref}(g,b)}$$

(Equation A11)

$$[Response\ Adjustment\ Factor](g,s,b) = \frac{[Single\ Particle\ Infection\ Probability](s,b)}{[Single\ Particle\ Infection\ Probability]_{ref}(g,b)}$$

S1.5. Absolute Infection Probability for Geographic Regions

Geographic regions, e.g., zip codes and census tracts, are often used when reporting epidemiological data and defining outbreak response zones, e.g., quarantine and/or vaccination. For this case, we define region *r* as a type of group and **Equation A7** can be rewritten as **Equation A12** where the reference exposure is defined by **Equation A13**.

(Equation A12)

$$[Infection\ Probability](r) \approx [Total\ Particles\ Released] \times \frac{\sum_{b=1}^{TB} \begin{pmatrix} [Release\ Probability](b) \\ \cdot\ [Single\ Particle\ Infection\ Probability]_{ref}(r,b) \\ \cdot\ [Adjustment\ Factor](r,b) \\ \cdot\ [Normalized\ TSIAC](r,b) \end{pmatrix}}{[Area](r)}$$

(Equation A13)

$$[Exposure]_{ref}(r,b) = \frac{[Total\ Particles\ Released] \cdot [Release\ Probability](b) \cdot [Normalized\ TSIAC](r,b)}{[Area](r)}$$

When considering outdoor plumes of infectious particles, we adapt the Regional Shelter Analysis (RSA) methodology to assign each location (subgroup *s*) a "protection factor" which is defined as the ratio of the outdoor to indoor exposures. As shown in (2, 3); building protection factors depend only on the building operating conditions, environmental parameters, and the particle type. Thus, for a given particle type, the assigned protection factors are identical to the inverse of the $[Exposure\ Adjustment\ Factor](r,s,b)$ where $[Exposure]_{ref}(r,b)$ is the outdoor time-integrated air concentration of *b*-type particles during the passage of the airborne infectious plume over region *r*.

S1.6. Relative Infection Probability for Geographic Regions

Given a plume of airborne infectious particles from a single source, then **Equation A12** implies **Equation A14** when a single particle type dominates the exposures. **Equation A14** does not depend on the specific release or the infectivity of individual particles. When the two regions are similar (e.g., both *r* and r_{ref} are residential areas with similar demographics) the adjustment factor ratio is unity. We demonstrate the utility of **Equation A14** in the *4. Results* and *5. Discussion and Conclusions* sections.

(Equation A14)

$$[Relative\ Infection\ Probability](r,b) = \frac{[Infection\ Probability](r,b)}{[Infection\ Probability](r_{ref},b)} = \left(\frac{[Normalized\ TSIAC](r,b)}{[Normalized\ TSIAC](r_{ref},b)}\right) \cdot \left(\frac{[Area](r_{ref})}{[Area](r)}\right) \cdot \left(\frac{[Adjustment\ Factor](r,b)}{[Adjustment\ Factor](r_{ref},b)}\right)$$

S1.7. Extrapolating Regional Infection Probabilities

When a clear case of region-to-region airborne disease transmission has been identified and a single particle type dominates the infections, **Equation A16**, derived from **Equations A15(a-b)**, estimates an effective source term for each infectious person in the source region.

(Equation A15a)

$$[Infections](r_{ref}, b)$$

$$= [Infection\ Probability](r_{ref}, b) \cdot [Area](r_{ref}) \cdot [Population\ Density](r_{ref})$$

$$\approx [Total\ Particles\ Released] \cdot [Release\ Probability](b) \cdot [Normalized\ TSIAC](r_{ref}, r_{source\ 1}, b) \cdot [Single\ Particle\ Infection\ Probability]_{ref}(r_{ref}, b) \cdot [Adjustment\ Factor](r_{ref}, b) \cdot [Population\ Density](r_{ref})$$

(Equation A15b)

$$\begin{pmatrix} [Total\ Particles\ Released] \cdot [Release\ Probability](b) \\ \cdot [Single\ Particle\ Infection\ Probability]_{ref}(r_{ref}, b) \\ \cdot [Adjustment\ Factor](r_{ref}, b) \end{pmatrix} \approx \frac{[Infections](r_{ref}, b)}{[Normalized\ TSIAC](r_{ref}, r_{source\ 1}, b) \cdot [Population\ Density](r_{ref})}$$

(Equation A16)

$$[Effective\ Source\ Term](r_{ref}, r_{source\ 1}, b)$$

$$\equiv \frac{\begin{pmatrix} [Total\ Particles\ Released] \cdot [Release\ Probability](b) \\ \cdot [Single\ Particle\ Infection\ Probability]_{ref}(r_{ref}, b) \\ \cdot [Adjustment\ Factor](r_{ref}, b) \end{pmatrix}}{[Infectious\ People](r_{source\ 1})}$$

$$= \frac{[Infection\ Probability](r_{ref}, b) \cdot [Area](r_{ref})}{[Normalized\ TSIAC](r_{ref}, r_{source\ 1}, b) \cdot [Infectious\ People](r_{source\ 1})}$$

Given the effective source term (**Equation A16**), the infection rates in other regions and times can then be estimated with **Equation A17a**. Alternately, **Equation A17b** can be used without the need to calculate the intermediate "effective source" quantity. The new term, the source adjustment factor, is introduced which adjusts for the number of airborne infectious particles emitted, e.g., a reduction in cough-emitted infectious particles due to use of respiratory masks. As with **Equation A14**, the reference and source regions disease adjustment factor may also be similar, i.e., their ratio may be unity, if buildings and demographics are similar in both source and target regions.

(Equation A17a)

$$[Infection\ Probability](r,b) = \frac{\begin{pmatrix}[Effective\ Source\ Term](r_{ref}, r_{source\ 1}, b) \\ \cdot\ [Normalized\ TSIAC](r, r_{source\ 2}, b) \\ \cdot\ [Infectious\ People](r_{source\ 2})\end{pmatrix}}{[Area](r)} \cdot \left(\frac{[Adjustment\ Factor](r,b)}{[Adjustment\ Factor](r_{ref},b)}\right) \cdot \left(\frac{[Source\ Adjustment\ Factor](r_{source\ 2},b)}{[Source\ Adjustment\ Factor](r_{source\ 1},b)}\right)$$

(Equation A17b)

$$[Infection\ Probability](r,b) = [Infection\ Probability](r_{ref}) \cdot \left(\frac{[Normalized\ TSIAC](r, r_{source\ 2}, b)}{[Normalized\ TSIAC](r_{ref}, r_{source\ 1}, b)}\right) \cdot \left(\frac{[Infectious\ People](r_{source\ 2})}{[Infectious\ People](r_{source\ 1})}\right) \cdot \left(\frac{[Adjustment\ Factor](r,b)}{[Adjustment\ Factor](r_{ref},b)}\right) \cdot \left(\frac{[Source\ Adjustment\ Factor](r_{source\ 2},b)}{[Source\ Adjustment\ Factor](r_{source\ 1},b)}\right) \cdot \left(\frac{[Area](r_{ref})}{[Area](r)}\right)$$

S1.8. Relationship to Disease and Other Metrics

The Supplemental Material equations presented up to this point focus on infection probability. However, not all infections result in disease. In addition, other metrics, such as probability of needing medical resources, may also be of interest. When the probability of the metric of interest, e.g., disease, can be linearly related to exposure, see **Equation A18**, then it is straightforward to adapt the prior equations for the metric of interest by replacing $[Infection\ Probabilty](p)$ with $[Metric\ of\ Interest\ Probability](p)$. We note than while $[Single\ Particle\ Metric\ of\ Interest\ Probability](p,b)$ can take any value and vary by individual and/or particle type, the value for a specific individual and particle type cannot change. We note that the adjustment factors can vary by metric.

*The relative incidence of multiple metrics of interest, such as infection and disease are the same since **Equations A14** and **A17** are unchanged by this substitution.*

(Equation A18)

$$[Metric\ of\ Interest\ Probability](p) = \sum_{b=1}^{TB}\left([Exposure](p,b) \cdot [Single\ Particle\ Probability\ for\ Metric\ of\ Interest](p,b)\right)$$

Supplemental Material S2:
Outdoor Normalized Time and Space Integrated Air Concentrations

Michael B Dillon

Outdoor normalized time and space integrated air concentration (Normalized TSIAC) values are a key component in our estimation of the outdoor Regional Relative Risk relationship with distance discussed in the main text. In this Supplemental Material, we describe how these values were calculated. For context, we also provide absolute and relative infection probabilities for a wider range of input parameter values than discussed in the main text. For ease of reference, we repeat here **Table B1**, which is also provided in the main text.

We use the Lawrence Livermore National Laboratory Atmospheric Data Assimilation and Parameterization Techniques (ADAPT) and Lagrangian Operational Dispersion Integrator (LODI) meteorological and atmospheric dispersion models to calculate outdoor normalized time and space integrated air concentrations (4, 5). The LODI/ADAPT model accuracy and validation are discussed in **S3**, *Atmospheric Dispersion Models* section.

We consider a suite of atmospheric conditions, **Table B1**, which were chosen to span a reasonably wide, but not comprehensive, range of common atmospheric conditions. The atmospheric conditions were held constant during the plume passage. Following this table, we provide the methodology and specific modeling assumptions used.

Tables B2(a-b) to **B5(a-b)** provide the ADAPT/LODI predicted outdoor Normalized TSIAC as a function of distance from an emission source, atmospheric conditions, and airborne loss rate. The Normalized TSIAC values are specified for both discs and circle arcs, see **Figure B1**, at distances ranging from 50 m to 20 km. Each look-up table corresponds to a single airborne (infectivity) loss rate (0, 0.1, 1, or 10 h^{-1} loss rates were modeled). Each table column corresponds to 1 of 7 commonly encountered wind speed and atmospheric stability combinations as specified in **Table B1**.

For context, **Figures B2** to **B5** provide downwind, upper bound estimates for two cases: (i) the average per-person, single particle, absolute infection probability (breathing rate = $2x10^{-4}$ m^3 s^{-1}) and (ii) the corresponding urban area infections. **Figures B6** to **B9** provide Relative Regional Risk (relative infection probabilities relative to 1 km disc or arc values). Each figure corresponds to a single airborne (infectivity) loss rate.

We modeled the downwind impacts assuming:

- The release quantity is one (effective) particle.
- All particles have 1 μm aerodynamic diameter.
- The released particle has a constant probability of being emitted from a point within a 1 hr period.
- Gravitational settling is the only deposition mechanism considered. The inclusion of other deposition mechanisms including (but not limited to) Brownian diffusion, rainout, impaction, and interception would all serve to reduce the modeled air concentrations and so our neglect of these mechanisms is consistent with the intent of providing an upper bound on the number of downwind infections.
- 4 different 1st order airborne loss rates (in addition to gravitational settling) are considered: 0, 0.1, 1, and 10 h^{-1}. These airborne loss rates are used to characterize the effects of airborne loss of particle infectivity.
- Resuspension (the re-emission of deposited material back into the atmosphere) is neglected.
- Flat terrain with a surface roughness of 0.1 m corresponding to a suburban setting. In forested and downtown regions, the earth's surface is typically rougher – resulting in lower surface air concentrations during stable and neutral atmospheric conditions.
- The modeled wind blew from the west (270°) to the east with no vertical or horizontal variation in wind direction (modeled wind speeds increase with height above ground).

Downwind concentrations were predicted using 2 modeling grids. The first had a 30 km horizontal extent and 100 m horizontal resolution grid cells. The second had a 1.5 km horizontal extent and 6 m horizontal resolution grid cells.

For each case, LODI was run with 1,000,000 marker particles[4] to calculate the (ensemble) average surface (lowest 20 m) normalized air concentrations integrated over the entire plume passage (i.e., until no marker particles remain in the modeling domain) for each model grid cell. For each atmospheric condition, the following procedure was used to calculate the normalized space and time integrated air concentration provided in **Tables B2(a-b)** to **B5(a-b)**.

First, we developed an interpolation function for each modeling grid using the MATLAB *griddedInterpolant* function configured to return either the value at the nearest sample grid point to the requested location (if the requested location is within the sample grid) or zero (if the requested location is outside the sample grid).

Second, we calculated the normalized time integrated air concentrations for a fixed set of radial distances by numerically integrating previously developed interpolation functions (using the MATLAB *integral* and *integral2* functions, as appropriate) for (i) a disk and (ii) circle arc, both centered on the release. For the 1.5 km extent grid, the distances considered were 50 m to 1,100 m at 50 m increments. For the 30 km extent grid, the distances considered were 2,000 m to 20,000 m at 1,000 m increments.

Third, we developed a second, linear interpolation function using the *griddedInterpolant* function from the distances considered and the normalized time integrated air concentrations calculated in step 2. This function was used for remainder of the analysis.

[4] These computational marker particles are a large sample from the possible particles emitted and are used in estimating downwind concentrations along with the prescribed contaminant emission amount. These particles do NOT directly represent individual physical aerosols.

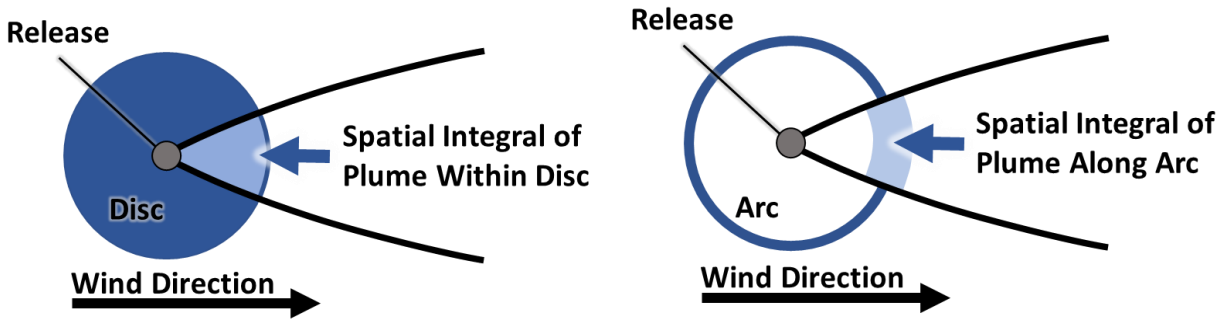

Figure B1. Illustration of airborne exposure (plume) integrated over a (left) a disc and (right) along a circle arc, both centered at the release point.

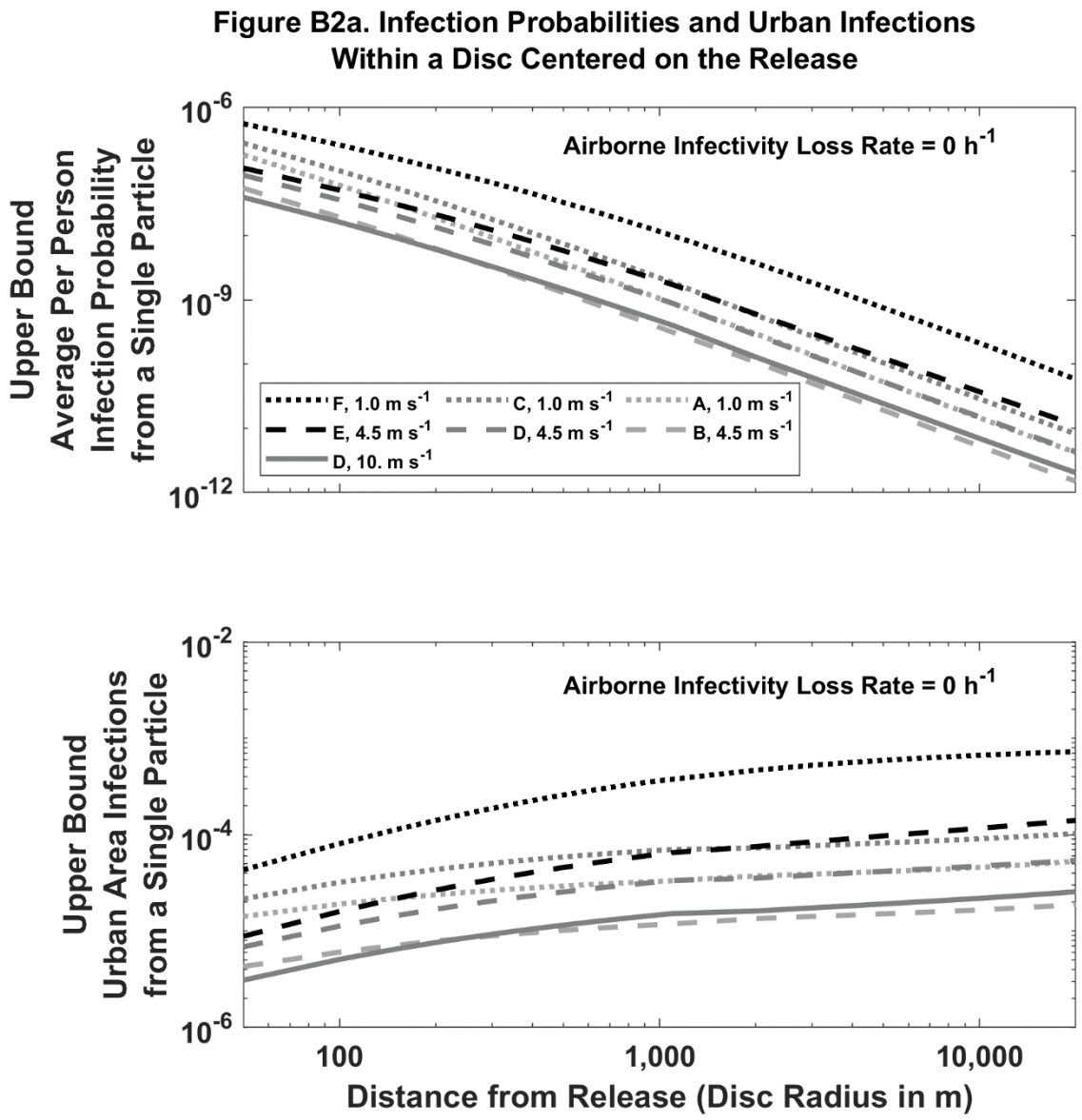

Figure B2a. Predicted absolute infection probabilities and infections by distance, wind speed and atmospheric stability for a single airborne particle with 0 h^{-1} airborne loss of infectivity. Legend indicates Pasquill-Gifford-Turner atmospheric stability class (A to F) and the 10 m agl wind speed. Individual person infection probability (top panels) is dimensionless. Urban area infections (bottom panels) assumes a uniform population density of 0.01 people m^{-2} and has dimensions of people.

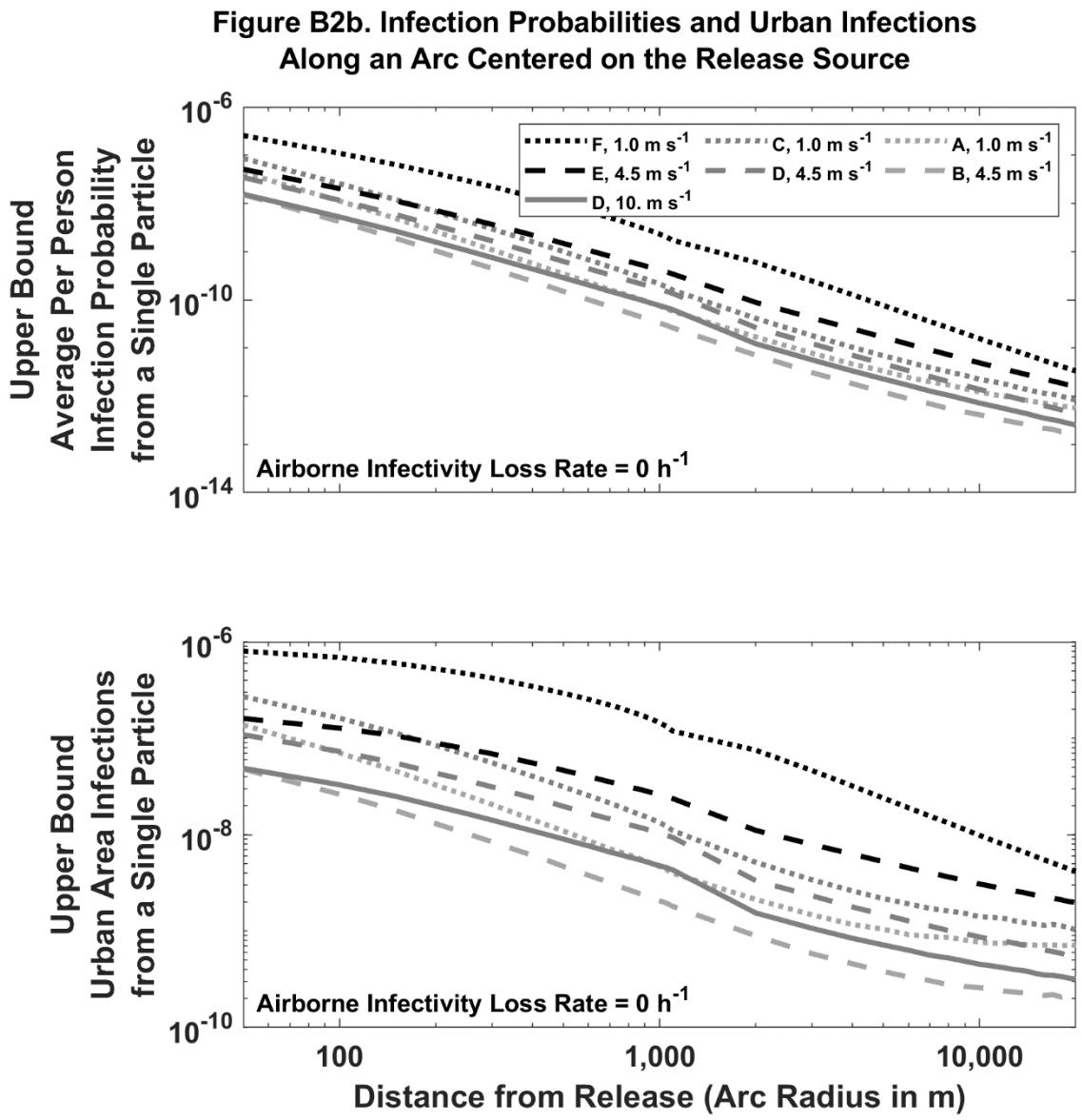

Figure B2b. Predicted absolute infection probabilities and infections by distance, wind speed and atmospheric stability for a single airborne particle with 0 h^{-1} airborne loss of infectivity. Legend indicates Pasquill-Gifford-Turner atmospheric stability class (A to F) and the 10 m agl wind speed. Individual person infection probability (top panels) is dimensionless. Urban area infections (bottom panels) assumes a uniform population density of 0.01 people m^{-2} and has dimensions of people m^{-1}.

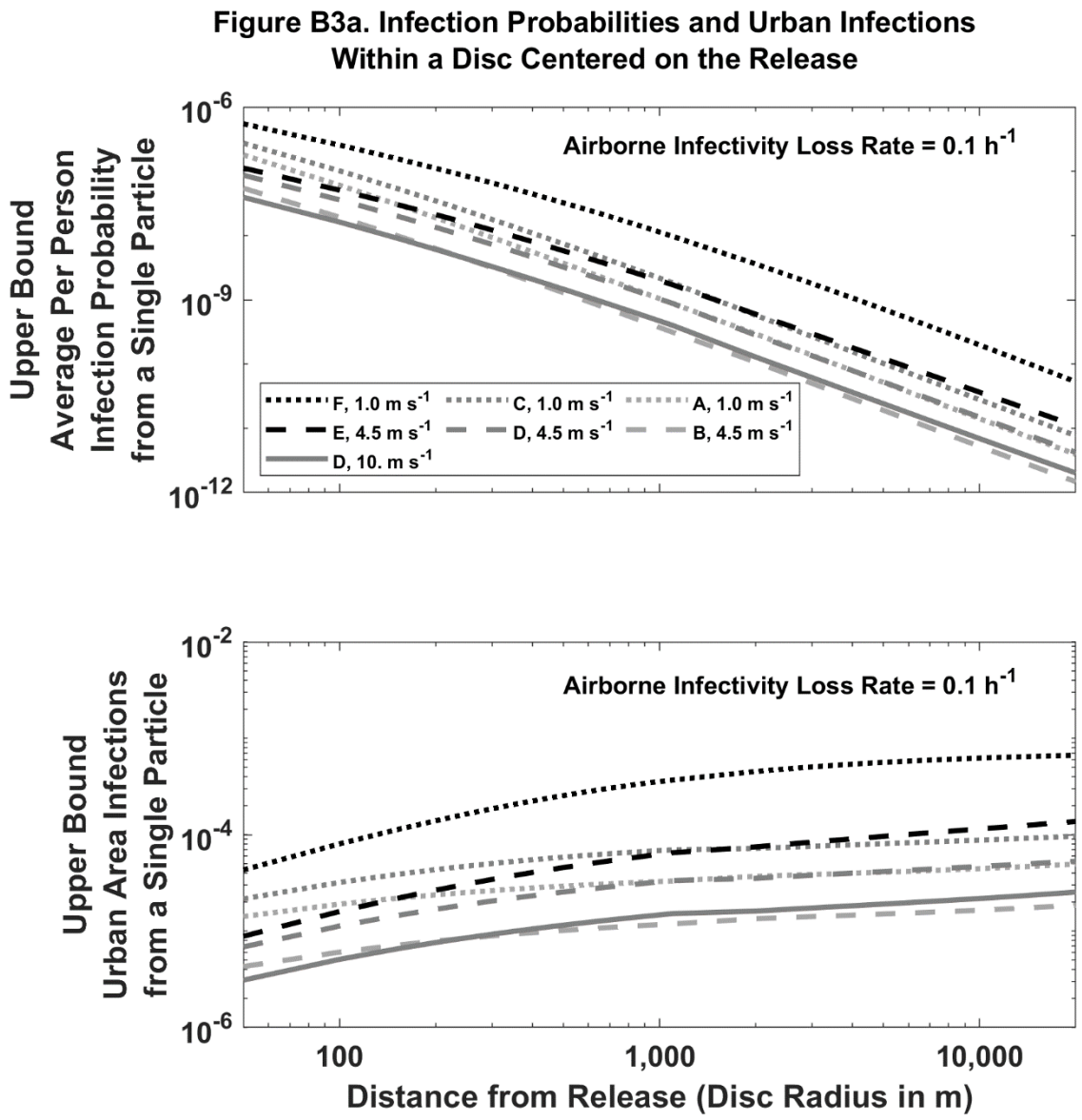

Figure B3a. Predicted absolute infection probabilities and infections by distance, wind speed and atmospheric stability for a single airborne particle with 0.1 h^{-1} airborne loss of infectivity. Legend indicates Pasquill-Gifford-Turner atmospheric stability class (A to F) and the 10 m agl wind speed. Individual person infection probability (top panels) is dimensionless. Urban area infections (bottom panels) assumes a uniform population density of 0.01 people m^{-2} and has dimensions of people.

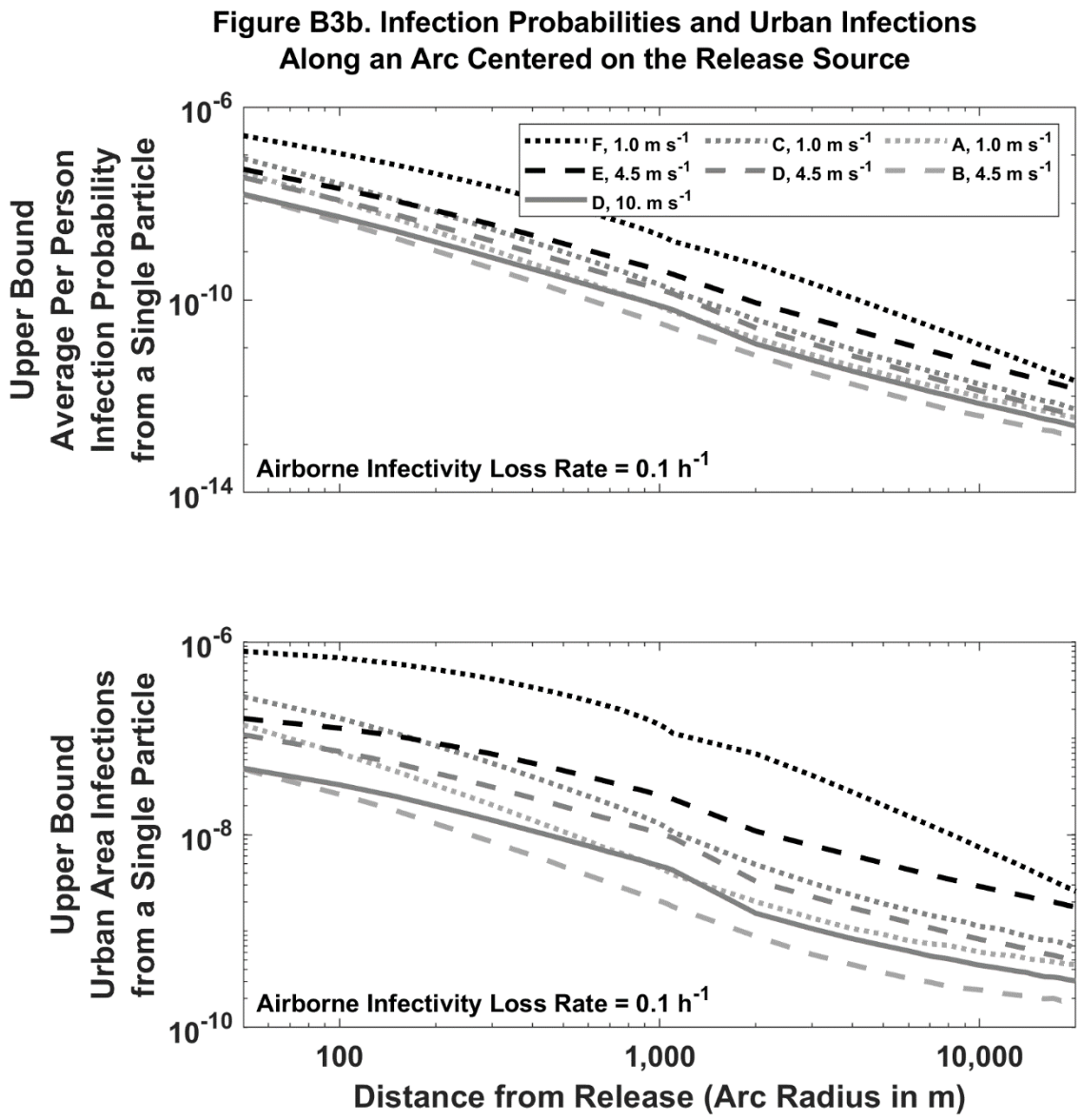

Figure B3b. Predicted absolute infection probabilities and infections by distance, wind speed and atmospheric stability for a single airborne particle with 0.1 h^{-1} airborne loss of infectivity. Legend indicates Pasquill-Gifford-Turner atmospheric stability class (A to F) and the 10 m agl wind speed. Individual person infection probability (top panels) is dimensionless. Urban area infections (bottom panels) assumes a uniform population density of 0.01 people m^{-2} and has dimensions of people m^{-1}.

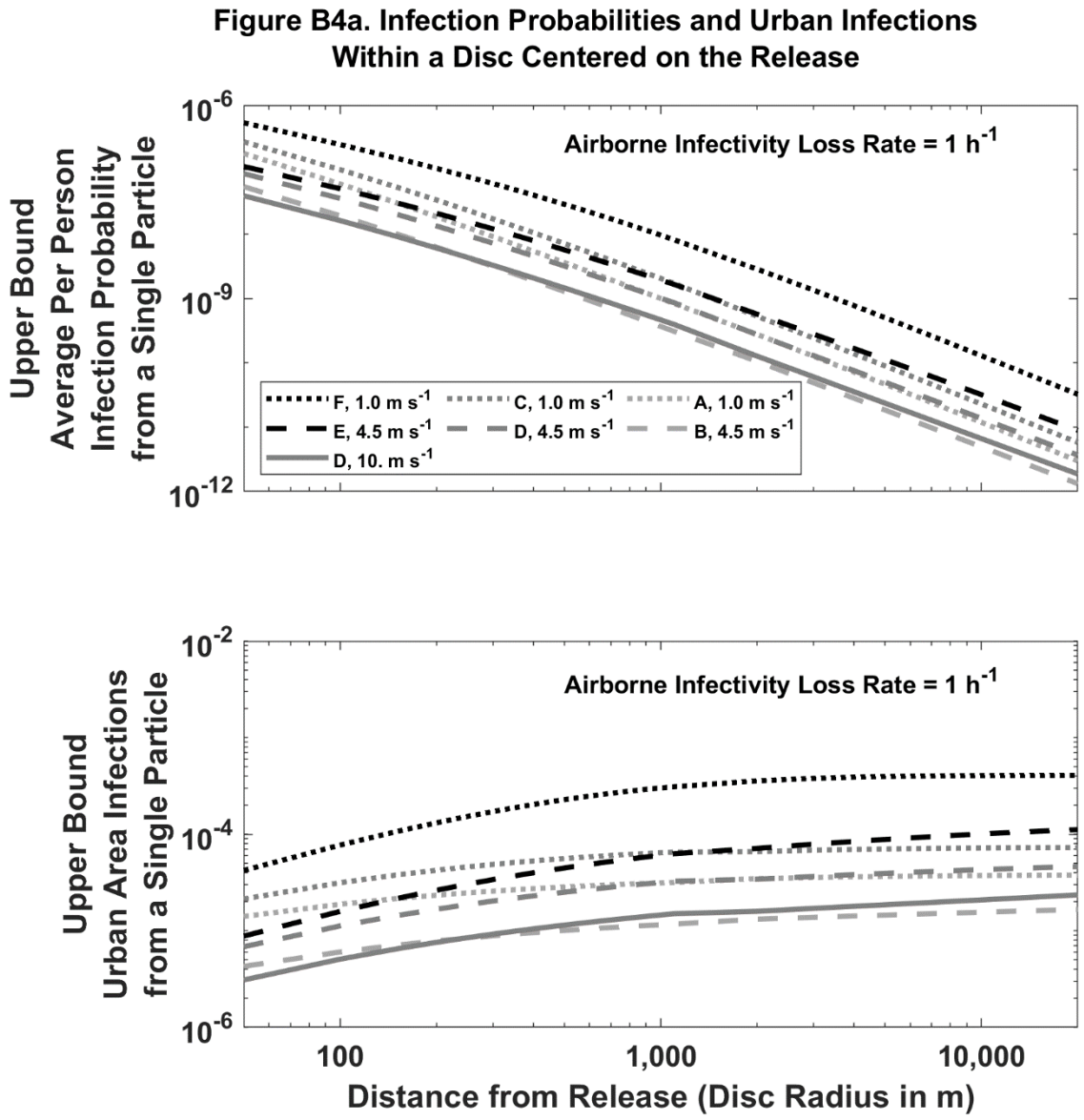

Figure B4a. Predicted absolute infection probabilities and infections by distance, wind speed and atmospheric stability for a single airborne particle with 1 h^{-1} airborne loss of infectivity. Legend indicates Pasquill-Gifford-Turner atmospheric stability class (A to F) and the 10 m agl wind speed. Individual person infection probability (top panels) is dimensionless. Urban area infections (bottom panels) assumes a uniform population density of 0.01 people m^{-2} and has dimensions of people.

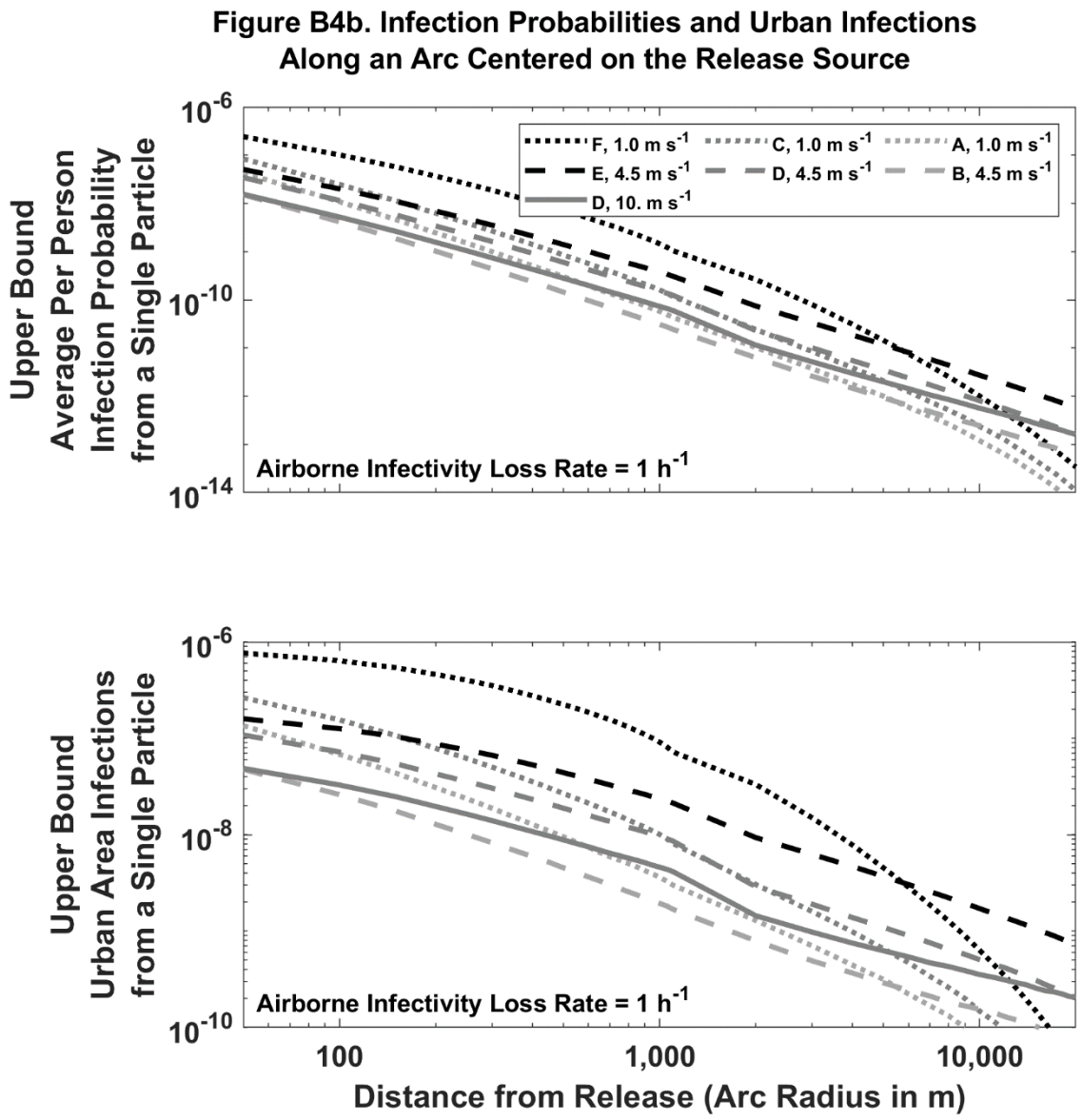

Figure B4b. Predicted absolute infection probabilities and infections by distance, wind speed and atmospheric stability for a single airborne particle with 1 h^{-1} airborne loss of infectivity. Legend indicates Pasquill-Gifford-Turner atmospheric stability class (A to F) and the 10 m agl wind speed. Individual person infection probability (top panels) is dimensionless. Urban area infections (bottom panels) assumes a uniform population density of 0.01 people m^{-2} and has dimensions of people m^{-1}.

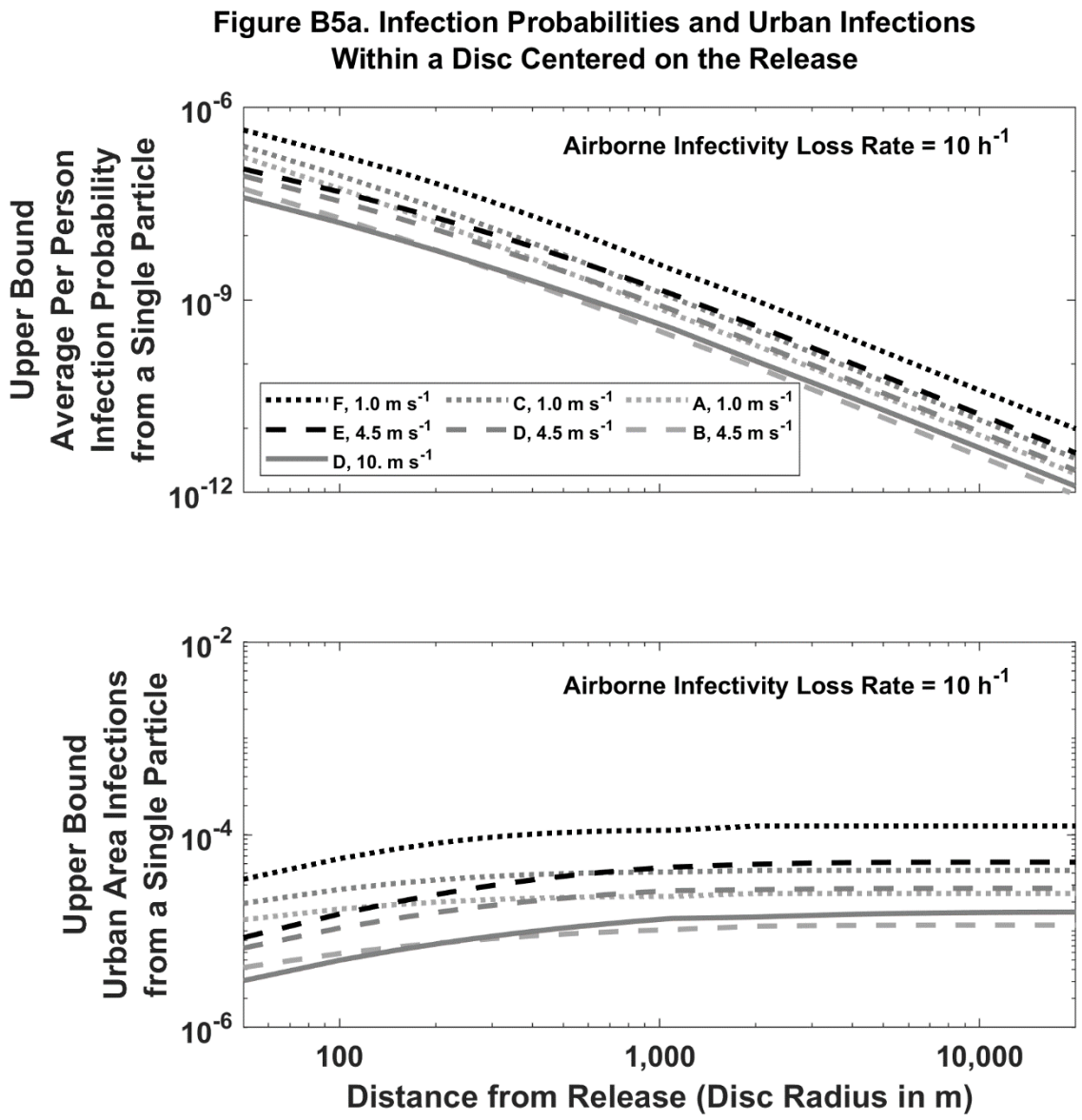

Figure B5a. Predicted absolute infection probabilities and infections by distance, wind speed and atmospheric stability for a single airborne particle with 10 h^{-1} airborne loss of infectivity. Legend indicates Pasquill-Gifford-Turner atmospheric stability class (A to F) and the 10 m agl wind speed. Individual person infection probability (top panels) is dimensionless. Urban area infections (bottom panels) a uniform population density of 0.01 people m^{-2} and has dimensions of people.

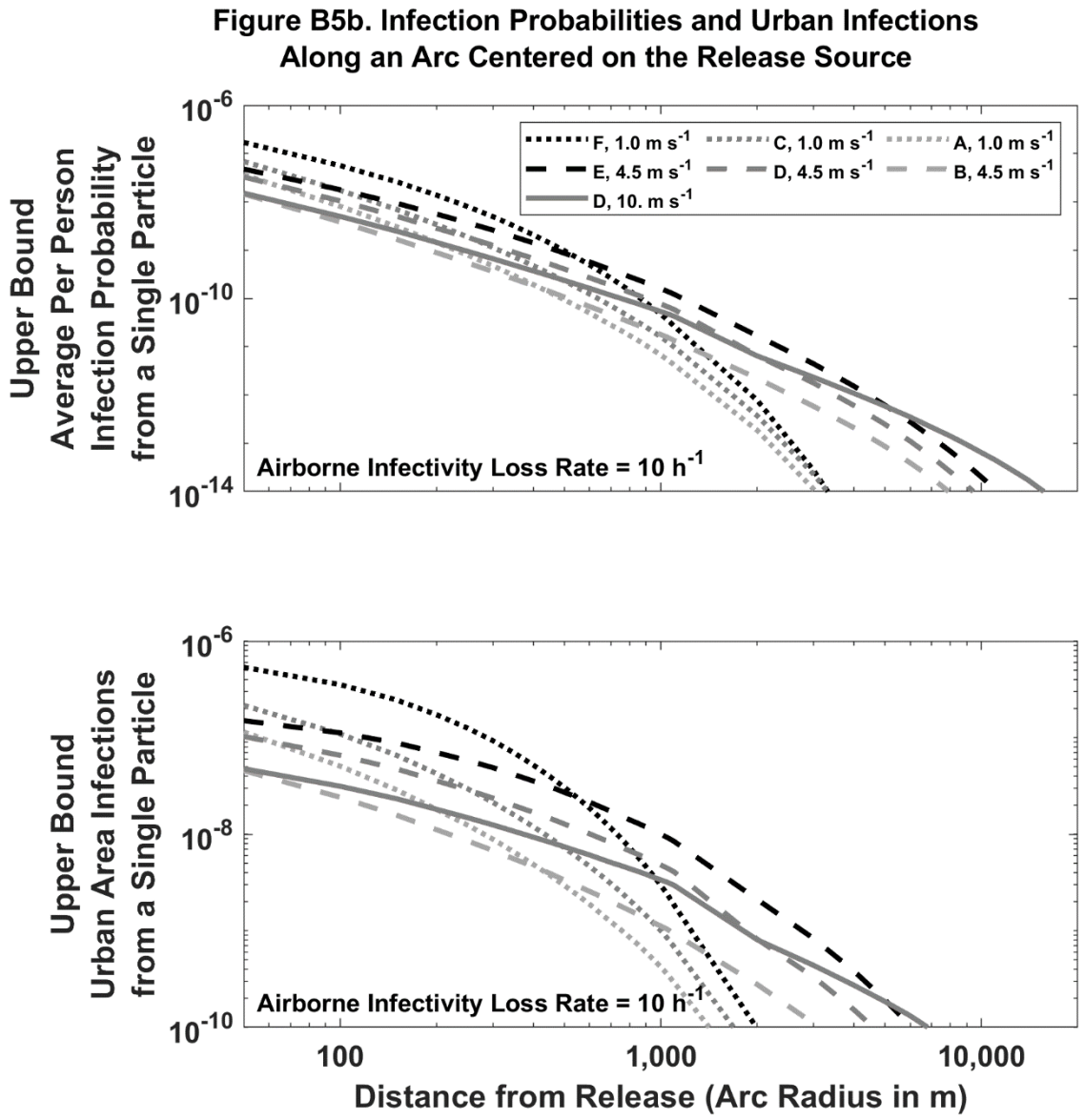

Figure B5b. Predicted absolute infection probabilities and infections by distance, wind speed and atmospheric stability for a single airborne particle with 10 h^{-1} airborne loss of infectivity. Legend indicates Pasquill-Gifford-Turner atmospheric stability class (A to F) and the 10 m agl wind speed. Individual person infection probability (top panels) is dimensionless. Urban area infections (bottom panels) a uniform population density of 0.01 people m^{-2} and has dimensions of people m^{-1}.

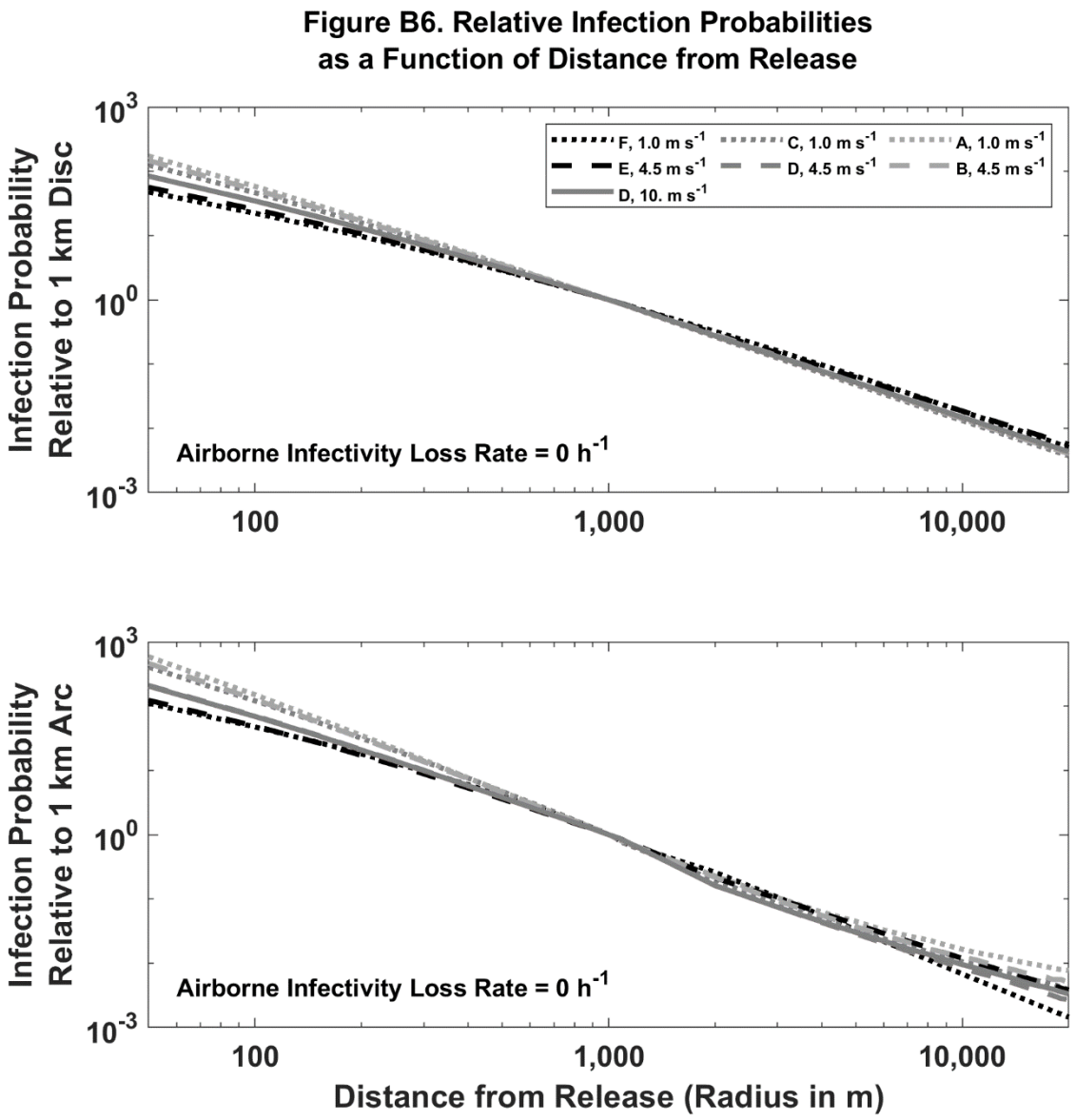

Figure B6. Predicted relative infection probabilities by distance, wind speed and atmospheric stability for a single airborne particle with 0 h^{-1} airborne loss of infectivity. Legend indicates Pasquill-Gifford-Turner atmospheric stability class (A to F) and the 10 m agl wind speed. Relative infection probability is dimensionless.

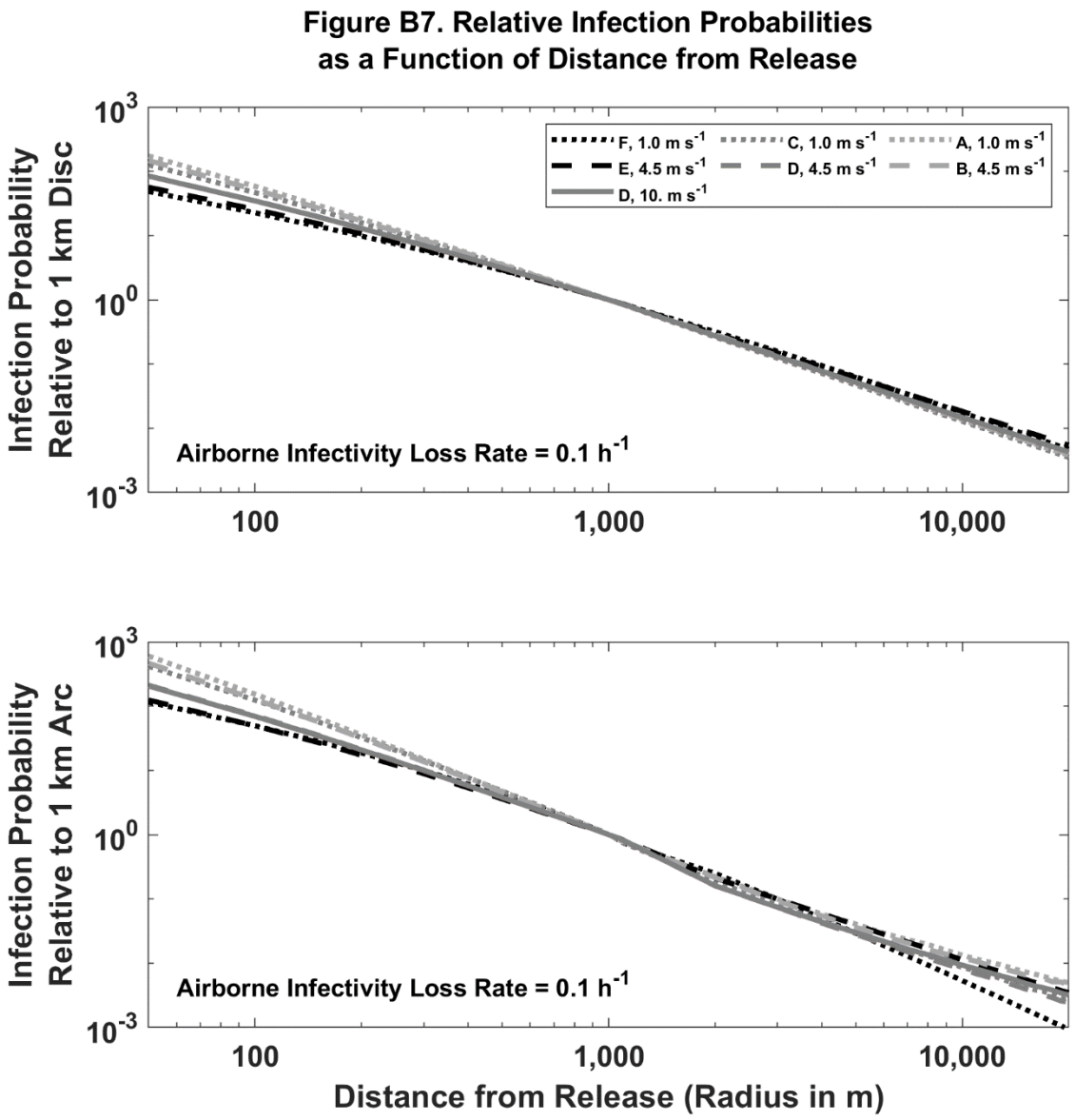

Figure B7. Predicted relative infection probabilities by distance, wind speed and atmospheric stability for a single airborne particle with 0.1 h^{-1} airborne loss of infectivity. Legend indicates Pasquill-Gifford-Turner atmospheric stability class (A to F) and the 10 m agl wind speed. Relative infection probability is dimensionless.

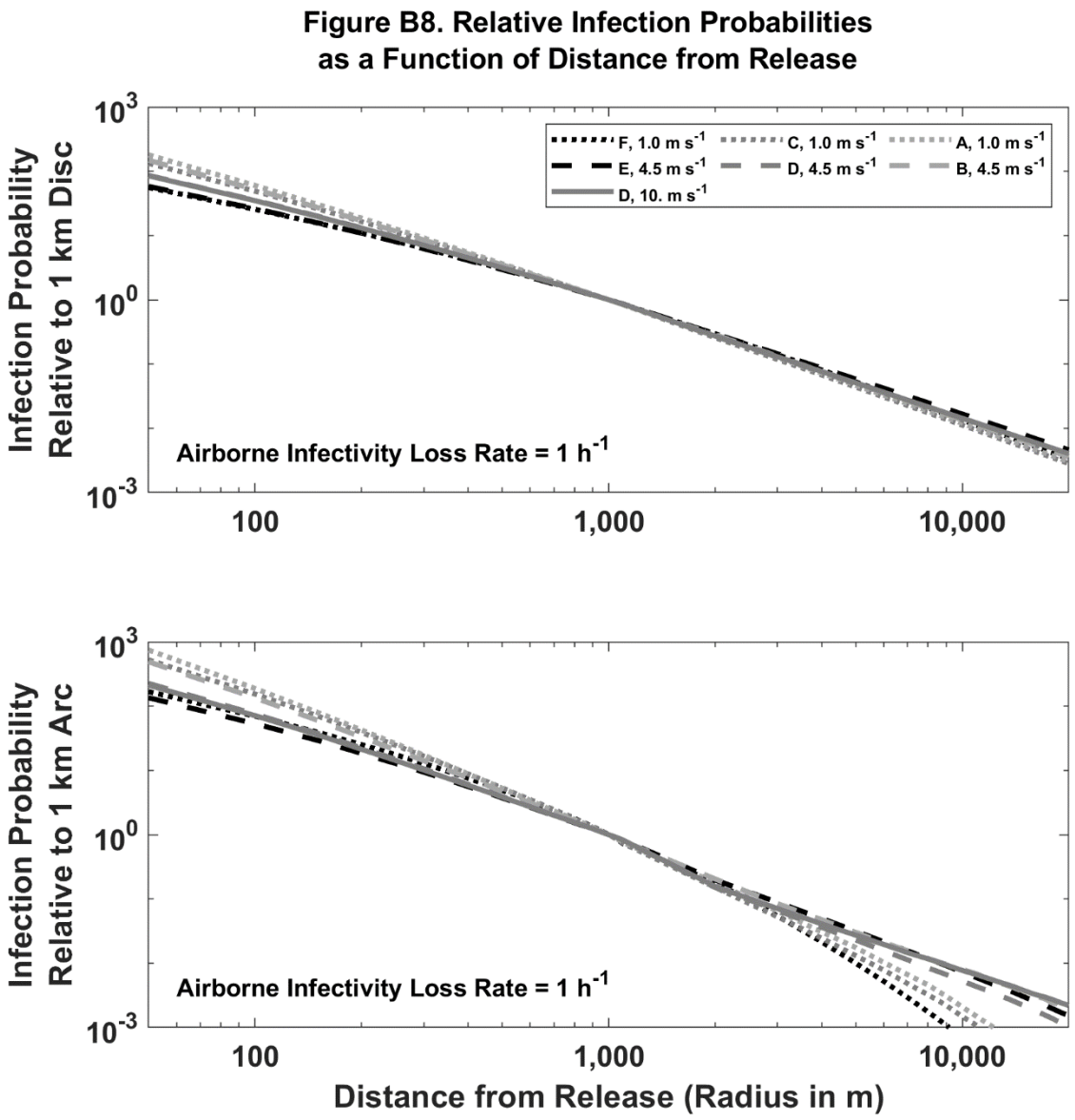

Figure B8. Predicted relative infection probabilities by distance, wind speed and atmospheric stability for a single airborne particle with 1 h^{-1} airborne loss of infectivity. Legend indicates Pasquill-Gifford-Turner atmospheric stability class (A to F) and the 10 m agl wind speed. Relative infection probability is dimensionless.

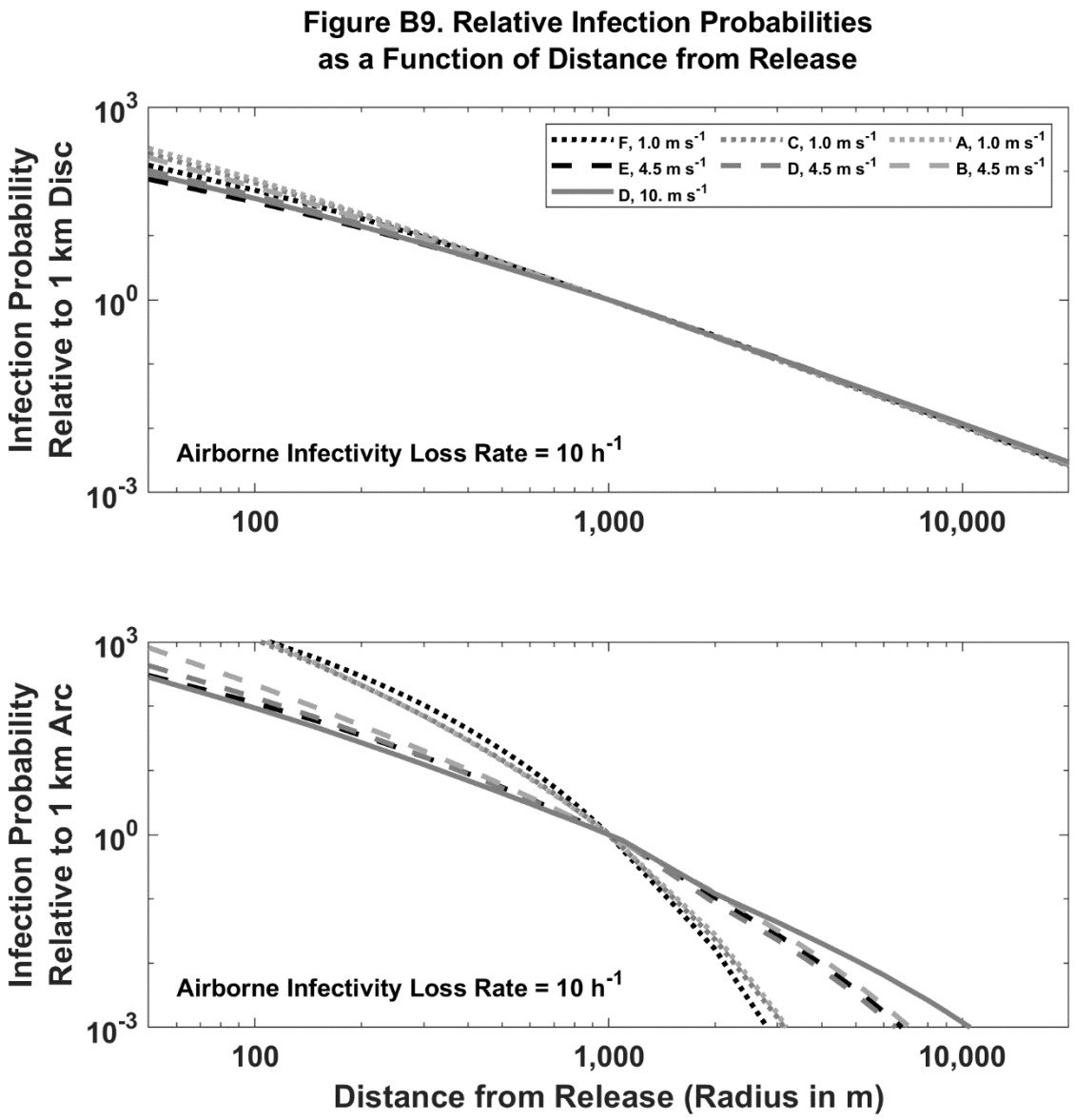

Figure B9. Predicted relative infection probabilities by distance, wind speed and atmospheric stability for a single airborne particle with 10 h^{-1} airborne loss of infectivity. Legend indicates Pasquill-Gifford-Turner atmospheric stability class (A to F) and the 10 m agl wind speed. Relative infection probability is dimensionless.

Table B1. Summary of modeled atmospheric conditions.

Qualitative Description	Stability Class (MO Length in m)	Wind Speed at 10 m above ground level in m s^{-1}	Boundary Layer Height in m
Clear, cold night with light winds	F (25)	1.0	300
Clear night with gentle breeze	E (50)	4.5	500
Overcast with light winds	C (-50)	1.0	1,000
Overcast with gentle breeze	D (∞)	4.5	800
Overcast with strong breeze	D (∞)	10	800
Clear day with gentle breeze	B (-25)	4.5	1,200
Clear, hot day with light winds	A (-10)	1.0	1,500

Table B2a. Normalized Time and Space Integrated Particle Air Concentration for a Disc with the specified distance from the release assuming no airborne loss rate (λ_{decay} = 0 h^{-1}).

Distance Downwind (m)	Clear, cold night with light winds ($s\ m^{-1}$)	Clear night with gentle breeze ($s\ m^{-1}$)	Overcast with light winds ($s\ m^{-1}$)	Overcast with gentle winds ($s\ m^{-1}$)	Overcast with strong winds ($s\ m^{-1}$)	Clear day with gentle winds ($s\ m^{-1}$)	Clear, hot day with light winds ($s\ m^{-1}$)
50	2.2E+01	4.4E+00	1.1E+01	3.4E+00	1.5E+00	2.1E+00	7.1E+00
100	4.0E+01	8.0E+00	1.6E+01	5.6E+00	2.5E+00	3.0E+00	9.5E+00
150	5.6E+01	1.1E+01	1.9E+01	7.2E+00	3.3E+00	3.6E+00	1.1E+01
200	7.0E+01	1.3E+01	2.2E+01	8.4E+00	3.8E+00	3.9E+00	1.2E+01
250	8.3E+01	1.5E+01	2.4E+01	9.4E+00	4.3E+00	4.2E+00	1.3E+01
300	9.4E+01	1.7E+01	2.5E+01	1.0E+01	4.6E+00	4.5E+00	1.3E+01
350	1.0E+02	1.9E+01	2.6E+01	1.1E+01	5.0E+00	4.6E+00	1.4E+01
400	1.1E+02	2.0E+01	2.8E+01	1.2E+01	5.3E+00	4.8E+00	1.4E+01
450	1.2E+02	2.2E+01	2.9E+01	1.2E+01	5.5E+00	5.0E+00	1.4E+01
500	1.3E+02	2.3E+01	2.9E+01	1.3E+01	5.8E+00	5.1E+00	1.5E+01
550	1.4E+02	2.4E+01	3.0E+01	1.3E+01	6.0E+00	5.2E+00	1.5E+01
600	1.4E+02	2.5E+01	3.1E+01	1.4E+01	6.2E+00	5.3E+00	1.5E+01
650	1.5E+02	2.6E+01	3.1E+01	1.4E+01	6.4E+00	5.4E+00	1.5E+01
700	1.5E+02	2.7E+01	3.2E+01	1.4E+01	6.5E+00	5.5E+00	1.6E+01
750	1.6E+02	2.8E+01	3.2E+01	1.5E+01	6.7E+00	5.5E+00	1.6E+01
800	1.6E+02	2.9E+01	3.3E+01	1.5E+01	6.8E+00	5.6E+00	1.6E+01
850	1.7E+02	2.9E+01	3.3E+01	1.5E+01	7.0E+00	5.7E+00	1.6E+01
900	1.7E+02	3.0E+01	3.4E+01	1.6E+01	7.1E+00	5.7E+00	1.6E+01
950	1.8E+02	3.1E+01	3.4E+01	1.6E+01	7.2E+00	5.8E+00	1.6E+01
1,000	1.8E+02	3.1E+01	3.4E+01	1.6E+01	7.4E+00	5.8E+00	1.6E+01
1,050	1.8E+02	3.2E+01	3.5E+01	1.6E+01	7.5E+00	5.9E+00	1.7E+01
1,100	1.9E+02	3.3E+01	3.5E+01	1.7E+01	7.6E+00	5.9E+00	1.7E+01
2,000	2.3E+02	3.8E+01	3.6E+01	1.8E+01	8.1E+00	6.7E+00	1.9E+01
3,000	2.6E+02	4.2E+01	3.8E+01	1.9E+01	8.7E+00	7.1E+00	1.9E+01
4,000	2.8E+02	4.6E+01	4.0E+01	2.0E+01	9.2E+00	7.3E+00	2.0E+01
5,000	3.0E+02	4.8E+01	4.1E+01	2.1E+01	9.6E+00	7.5E+00	2.1E+01
6,000	3.1E+02	5.1E+01	4.2E+01	2.2E+01	9.9E+00	7.7E+00	2.1E+01
7,000	3.1E+02	5.3E+01	4.3E+01	2.2E+01	1.0E+01	7.9E+00	2.2E+01
8,000	3.2E+02	5.5E+01	4.4E+01	2.3E+01	1.0E+01	8.0E+00	2.2E+01
9,000	3.3E+02	5.7E+01	4.5E+01	2.3E+01	1.1E+01	8.2E+00	2.2E+01
10,000	3.3E+02	5.8E+01	4.5E+01	2.4E+01	1.1E+01	8.3E+00	2.3E+01
11,000	3.4E+02	6.0E+01	4.6E+01	2.4E+01	1.1E+01	8.4E+00	2.3E+01
12,000	3.4E+02	6.1E+01	4.7E+01	2.4E+01	1.1E+01	8.5E+00	2.4E+01
13,000	3.5E+02	6.2E+01	4.7E+01	2.5E+01	1.2E+01	8.7E+00	2.4E+01
14,000	3.5E+02	6.4E+01	4.8E+01	2.5E+01	1.2E+01	8.8E+00	2.4E+01
15,000	3.5E+02	6.5E+01	4.9E+01	2.6E+01	1.2E+01	8.9E+00	2.5E+01
16,000	3.5E+02	6.6E+01	4.9E+01	2.6E+01	1.2E+01	9.0E+00	2.5E+01
17,000	3.6E+02	6.7E+01	5.0E+01	2.6E+01	1.2E+01	9.1E+00	2.5E+01
18,000	3.6E+02	6.8E+01	5.0E+01	2.6E+01	1.2E+01	9.2E+00	2.6E+01
19,000	3.6E+02	6.9E+01	5.1E+01	2.7E+01	1.3E+01	9.3E+00	2.6E+01
20,000	3.6E+02	7.0E+01	5.1E+01	2.7E+01	1.3E+01	9.4E+00	2.7E+01

Table B2b. Normalized Time and Space Integrated Particle Air Concentration for a Circle Arc at the specified distance from the release assuming no airborne loss rate (λ_{decay} = 0 h^{-1}).

Distance Downwind (m)	Clear, cold night with light winds ($s\ m^{-2}$)	Clear night with gentle breeze ($s\ m^{-2}$)	Overcast with light winds ($s\ m^{-2}$)	Overcast with gentle winds ($s\ m^{-2}$)	Overcast with strong winds ($s\ m^{-2}$)	Clear day with gentle winds ($s\ m^{-2}$)	Clear, hot day with light winds ($s\ m^{-2}$)
50	4.0E-01	8.0E-02	1.4E-01	5.4E-02	2.4E-02	2.4E-02	6.9E-02
100	3.4E-01	6.4E-02	8.1E-02	3.6E-02	1.6E-02	1.3E-02	3.5E-02
150	3.0E-01	5.3E-02	5.6E-02	2.8E-02	1.2E-02	8.9E-03	2.3E-02
200	2.6E-01	4.5E-02	4.2E-02	2.2E-02	9.9E-03	6.5E-03	1.6E-02
250	2.3E-01	3.9E-02	3.4E-02	1.8E-02	8.3E-03	5.1E-03	1.3E-02
300	2.1E-01	3.4E-02	2.8E-02	1.6E-02	7.1E-03	4.2E-03	1.0E-02
350	1.9E-01	3.1E-02	2.3E-02	1.4E-02	6.2E-03	3.5E-03	8.5E-03
400	1.7E-01	2.8E-02	2.0E-02	1.2E-02	5.5E-03	3.1E-03	7.2E-03
450	1.6E-01	2.5E-02	1.8E-02	1.1E-02	5.0E-03	2.7E-03	6.2E-03
500	1.5E-01	2.3E-02	1.6E-02	9.8E-03	4.5E-03	2.3E-03	5.5E-03
550	1.4E-01	2.2E-02	1.4E-02	9.0E-03	4.1E-03	2.1E-03	4.9E-03
600	1.3E-01	2.0E-02	1.3E-02	8.3E-03	3.8E-03	1.9E-03	4.4E-03
650	1.2E-01	1.9E-02	1.2E-02	7.7E-03	3.5E-03	1.7E-03	3.9E-03
700	1.1E-01	1.8E-02	1.1E-02	7.3E-03	3.3E-03	1.6E-03	3.6E-03
750	1.0E-01	1.7E-02	9.8E-03	6.8E-03	3.1E-03	1.4E-03	3.3E-03
800	9.6E-02	1.6E-02	9.0E-03	6.4E-03	2.9E-03	1.3E-03	3.1E-03
850	9.0E-02	1.5E-02	8.3E-03	6.0E-03	2.8E-03	1.3E-03	2.9E-03
900	8.4E-02	1.4E-02	7.7E-03	5.8E-03	2.6E-03	1.2E-03	2.7E-03
950	7.8E-02	1.4E-02	7.2E-03	5.5E-03	2.5E-03	1.1E-03	2.5E-03
1,000	7.2E-02	1.3E-02	6.7E-03	5.2E-03	2.4E-03	1.0E-03	2.3E-03
1,050	6.7E-02	1.2E-02	6.1E-03	4.9E-03	2.3E-03	9.7E-04	2.2E-03
1,100	5.9E-02	1.2E-02	5.5E-03	4.7E-03	2.2E-03	9.0E-04	2.0E-03
2,000	3.8E-02	5.5E-03	2.6E-03	1.7E-03	7.7E-04	4.5E-04	1.1E-03
3,000	2.3E-02	4.0E-03	1.7E-03	1.2E-03	5.3E-04	2.9E-04	7.3E-04
4,000	1.6E-02	3.1E-03	1.3E-03	8.9E-04	4.2E-04	2.3E-04	5.9E-04
5,000	1.2E-02	2.6E-03	1.1E-03	7.4E-04	3.6E-04	1.9E-04	5.2E-04
6,000	9.5E-03	2.3E-03	9.6E-04	6.4E-04	3.2E-04	1.7E-04	4.6E-04
7,000	7.8E-03	2.0E-03	8.6E-04	5.6E-04	2.8E-04	1.5E-04	4.4E-04
8,000	6.6E-03	1.8E-03	8.1E-04	5.1E-04	2.6E-04	1.4E-04	4.3E-04
9,000	5.7E-03	1.7E-03	7.6E-04	4.7E-04	2.4E-04	1.3E-04	4.0E-04
10,000	4.9E-03	1.5E-03	7.0E-04	4.3E-04	2.3E-04	1.3E-04	3.8E-04
11,000	4.4E-03	1.4E-03	6.9E-04	4.1E-04	2.2E-04	1.3E-04	3.7E-04
12,000	3.9E-03	1.4E-03	6.7E-04	3.9E-04	2.1E-04	1.2E-04	3.7E-04
13,000	3.6E-03	1.3E-03	6.3E-04	3.7E-04	2.0E-04	1.2E-04	3.7E-04
14,000	3.2E-03	1.2E-03	6.1E-04	3.5E-04	1.9E-04	1.1E-04	3.6E-04
15,000	3.0E-03	1.2E-03	5.9E-04	3.3E-04	1.8E-04	1.1E-04	3.6E-04
16,000	2.7E-03	1.1E-03	5.7E-04	3.2E-04	1.7E-04	1.1E-04	3.6E-04
17,000	2.5E-03	1.1E-03	5.9E-04	3.1E-04	1.7E-04	1.1E-04	3.6E-04
18,000	2.4E-03	1.1E-03	5.7E-04	2.9E-04	1.7E-04	1.0E-04	3.5E-04
19,000	2.2E-03	1.0E-03	5.4E-04	2.8E-04	1.6E-04	1.1E-04	3.5E-04
20,000	2.1E-03	9.9E-04	5.2E-04	2.8E-04	1.6E-04	1.0E-04	3.6E-04

Table B3a. Normalized Time and Space Integrated Particle Air Concentration for a Disc with the specified distance from the release assuming airborne loss rate (λ_{decay} = 0.1 h^{-1}).

Distance Downwind (m)	Clear, cold night with light winds ($s\ m^{-1}$)	Clear night with gentle breeze ($s\ m^{-1}$)	Overcast with light winds ($s\ m^{-1}$)	Overcast with gentle winds ($s\ m^{-1}$)	Overcast with strong winds ($s\ m^{-1}$)	Clear day with gentle winds ($s\ m^{-1}$)	Clear, hot day with light winds ($s\ m^{-1}$)
50	2.2E+01	4.4E+00	1.1E+01	3.4E+00	1.5E+00	2.1E+00	7.1E+00
100	4.0E+01	8.0E+00	1.6E+01	5.6E+00	2.5E+00	3.0E+00	9.5E+00
150	5.6E+01	1.1E+01	1.9E+01	7.2E+00	3.3E+00	3.6E+00	1.1E+01
200	7.0E+01	1.3E+01	2.2E+01	8.4E+00	3.8E+00	3.9E+00	1.2E+01
250	8.2E+01	1.5E+01	2.4E+01	9.4E+00	4.3E+00	4.2E+00	1.3E+01
300	9.3E+01	1.7E+01	2.5E+01	1.0E+01	4.6E+00	4.5E+00	1.3E+01
350	1.0E+02	1.9E+01	2.6E+01	1.1E+01	5.0E+00	4.6E+00	1.4E+01
400	1.1E+02	2.0E+01	2.7E+01	1.2E+01	5.3E+00	4.8E+00	1.4E+01
450	1.2E+02	2.2E+01	2.8E+01	1.2E+01	5.5E+00	5.0E+00	1.4E+01
500	1.3E+02	2.3E+01	2.9E+01	1.3E+01	5.8E+00	5.1E+00	1.5E+01
550	1.3E+02	2.4E+01	3.0E+01	1.3E+01	6.0E+00	5.2E+00	1.5E+01
600	1.4E+02	2.5E+01	3.1E+01	1.4E+01	6.2E+00	5.3E+00	1.5E+01
650	1.5E+02	2.6E+01	3.1E+01	1.4E+01	6.3E+00	5.4E+00	1.5E+01
700	1.5E+02	2.7E+01	3.2E+01	1.4E+01	6.5E+00	5.5E+00	1.5E+01
750	1.6E+02	2.8E+01	3.2E+01	1.5E+01	6.7E+00	5.5E+00	1.6E+01
800	1.6E+02	2.8E+01	3.3E+01	1.5E+01	6.8E+00	5.6E+00	1.6E+01
850	1.7E+02	2.9E+01	3.3E+01	1.5E+01	7.0E+00	5.7E+00	1.6E+01
900	1.7E+02	3.0E+01	3.3E+01	1.6E+01	7.1E+00	5.7E+00	1.6E+01
950	1.7E+02	3.1E+01	3.4E+01	1.6E+01	7.2E+00	5.8E+00	1.6E+01
1,000	1.8E+02	3.1E+01	3.4E+01	1.6E+01	7.4E+00	5.8E+00	1.6E+01
1,050	1.8E+02	3.2E+01	3.5E+01	1.6E+01	7.5E+00	5.9E+00	1.6E+01
1,100	1.8E+02	3.2E+01	3.5E+01	1.7E+01	7.6E+00	5.9E+00	1.7E+01
2,000	2.3E+02	3.7E+01	3.6E+01	1.8E+01	8.1E+00	6.7E+00	1.8E+01
3,000	2.5E+02	4.2E+01	3.8E+01	1.9E+01	8.7E+00	7.1E+00	1.9E+01
4,000	2.7E+02	4.5E+01	3.9E+01	2.0E+01	9.1E+00	7.3E+00	2.0E+01
5,000	2.8E+02	4.8E+01	4.0E+01	2.1E+01	9.5E+00	7.5E+00	2.0E+01
6,000	2.9E+02	5.0E+01	4.1E+01	2.1E+01	9.9E+00	7.7E+00	2.1E+01
7,000	3.0E+02	5.2E+01	4.2E+01	2.2E+01	1.0E+01	7.8E+00	2.1E+01
8,000	3.0E+02	5.4E+01	4.3E+01	2.2E+01	1.0E+01	8.0E+00	2.2E+01
9,000	3.1E+02	5.6E+01	4.3E+01	2.3E+01	1.1E+01	8.1E+00	2.2E+01
10,000	3.1E+02	5.7E+01	4.4E+01	2.3E+01	1.1E+01	8.2E+00	2.2E+01
11,000	3.1E+02	5.9E+01	4.4E+01	2.4E+01	1.1E+01	8.4E+00	2.3E+01
12,000	3.2E+02	6.0E+01	4.5E+01	2.4E+01	1.1E+01	8.5E+00	2.3E+01
13,000	3.2E+02	6.1E+01	4.5E+01	2.4E+01	1.1E+01	8.6E+00	2.3E+01
14,000	3.2E+02	6.2E+01	4.6E+01	2.5E+01	1.2E+01	8.7E+00	2.3E+01
15,000	3.2E+02	6.4E+01	4.6E+01	2.5E+01	1.2E+01	8.8E+00	2.4E+01
16,000	3.3E+02	6.5E+01	4.7E+01	2.5E+01	1.2E+01	8.9E+00	2.4E+01
17,000	3.3E+02	6.6E+01	4.7E+01	2.6E+01	1.2E+01	9.0E+00	2.4E+01
18,000	3.3E+02	6.7E+01	4.8E+01	2.6E+01	1.2E+01	9.1E+00	2.4E+01
19,000	3.3E+02	6.8E+01	4.8E+01	2.6E+01	1.3E+01	9.2E+00	2.5E+01
20,000	3.3E+02	6.8E+01	4.8E+01	2.7E+01	1.3E+01	9.3E+00	2.5E+01

Table B3b. Normalized Time and Space Integrated Particle Air Concentration for a Circle Arc at the specified distance from the release assuming airborne loss rate (λ_{decay} = 0.1 h^{-1}).

Distance Downwind (m)	Clear, cold night with light winds ($s\ m^{-2}$)	Clear night with gentle breeze ($s\ m^{-2}$)	Overcast with light winds ($s\ m^{-2}$)	Overcast with gentle winds ($s\ m^{-2}$)	Overcast with strong winds ($s\ m^{-2}$)	Clear day with gentle winds ($s\ m^{-2}$)	Clear, hot day with light winds ($s\ m^{-2}$)
50	4.0E-01	8.0E-02	1.3E-01	5.4E-02	2.4E-02	2.4E-02	6.9E-02
100	3.4E-01	6.4E-02	8.0E-02	3.6E-02	1.6E-02	1.3E-02	3.5E-02
150	3.0E-01	5.3E-02	5.6E-02	2.8E-02	1.2E-02	8.9E-03	2.3E-02
200	2.6E-01	4.4E-02	4.2E-02	2.2E-02	9.9E-03	6.5E-03	1.6E-02
250	2.3E-01	3.9E-02	3.3E-02	1.8E-02	8.2E-03	5.1E-03	1.3E-02
300	2.1E-01	3.4E-02	2.8E-02	1.6E-02	7.1E-03	4.2E-03	1.0E-02
350	1.9E-01	3.1E-02	2.3E-02	1.4E-02	6.2E-03	3.5E-03	8.4E-03
400	1.7E-01	2.8E-02	2.0E-02	1.2E-02	5.5E-03	3.1E-03	7.1E-03
450	1.5E-01	2.5E-02	1.7E-02	1.1E-02	4.9E-03	2.7E-03	6.1E-03
500	1.4E-01	2.3E-02	1.5E-02	9.8E-03	4.5E-03	2.3E-03	5.4E-03
550	1.3E-01	2.1E-02	1.4E-02	9.0E-03	4.1E-03	2.1E-03	4.8E-03
600	1.2E-01	2.0E-02	1.3E-02	8.3E-03	3.8E-03	1.9E-03	4.3E-03
650	1.1E-01	1.9E-02	1.1E-02	7.7E-03	3.5E-03	1.7E-03	3.8E-03
700	1.1E-01	1.7E-02	1.0E-02	7.2E-03	3.3E-03	1.6E-03	3.5E-03
750	1.0E-01	1.7E-02	9.6E-03	6.7E-03	3.1E-03	1.4E-03	3.3E-03
800	9.3E-02	1.6E-02	8.8E-03	6.3E-03	2.9E-03	1.3E-03	3.0E-03
850	8.6E-02	1.5E-02	8.1E-03	6.0E-03	2.8E-03	1.2E-03	2.8E-03
900	8.0E-02	1.4E-02	7.5E-03	5.7E-03	2.6E-03	1.2E-03	2.6E-03
950	7.5E-02	1.3E-02	7.0E-03	5.4E-03	2.5E-03	1.1E-03	2.4E-03
1,000	6.9E-02	1.3E-02	6.5E-03	5.1E-03	2.4E-03	1.0E-03	2.3E-03
1,050	6.3E-02	1.2E-02	6.0E-03	4.9E-03	2.3E-03	9.7E-04	2.1E-03
1,100	5.6E-02	1.2E-02	5.3E-03	4.6E-03	2.1E-03	8.9E-04	1.9E-03
2,000	3.5E-02	5.4E-03	2.4E-03	1.6E-03	7.6E-04	4.4E-04	1.0E-03
3,000	2.1E-02	3.9E-03	1.6E-03	1.1E-03	5.3E-04	2.9E-04	6.8E-04
4,000	1.4E-02	3.1E-03	1.2E-03	8.7E-04	4.2E-04	2.2E-04	5.3E-04
5,000	1.0E-02	2.5E-03	9.6E-04	7.2E-04	3.5E-04	1.9E-04	4.6E-04
6,000	7.8E-03	2.2E-03	8.3E-04	6.2E-04	3.1E-04	1.6E-04	4.0E-04
7,000	6.2E-03	1.9E-03	7.3E-04	5.4E-04	2.8E-04	1.5E-04	3.7E-04
8,000	5.2E-03	1.7E-03	6.7E-04	4.8E-04	2.6E-04	1.3E-04	3.6E-04
9,000	4.3E-03	1.6E-03	6.2E-04	4.5E-04	2.4E-04	1.3E-04	3.3E-04
10,000	3.7E-03	1.5E-03	5.6E-04	4.1E-04	2.2E-04	1.2E-04	3.0E-04
11,000	3.2E-03	1.4E-03	5.4E-04	3.8E-04	2.1E-04	1.2E-04	2.9E-04
12,000	2.8E-03	1.3E-03	5.1E-04	3.7E-04	2.0E-04	1.1E-04	2.8E-04
13,000	2.5E-03	1.2E-03	4.7E-04	3.5E-04	1.9E-04	1.1E-04	2.8E-04
14,000	2.2E-03	1.1E-03	4.4E-04	3.3E-04	1.9E-04	1.1E-04	2.6E-04
15,000	2.0E-03	1.1E-03	4.2E-04	3.1E-04	1.8E-04	1.0E-04	2.5E-04
16,000	1.8E-03	1.0E-03	4.0E-04	2.9E-04	1.7E-04	9.9E-05	2.5E-04
17,000	1.7E-03	1.0E-03	4.0E-04	2.8E-04	1.7E-04	1.0E-04	2.4E-04
18,000	1.5E-03	9.6E-04	3.8E-04	2.7E-04	1.6E-04	9.4E-05	2.3E-04
19,000	1.4E-03	9.2E-04	3.5E-04	2.5E-04	1.6E-04	9.9E-05	2.3E-04
20,000	1.3E-03	8.9E-04	3.3E-04	2.5E-04	1.5E-04	9.4E-05	2.3E-04

Table B4a. Normalized Time and Space Integrated Particle Air Concentration for a Disc with the specified distance from the release assuming airborne loss rate (λ_{decay} = 1 h^{-1}).

Distance Downwind (m)	Clear, cold night with light winds ($s\ m^{-1}$)	Clear night with gentle breeze ($s\ m^{-1}$)	Overcast with light winds ($s\ m^{-1}$)	Overcast with gentle winds ($s\ m^{-1}$)	Overcast with strong winds ($s\ m^{-1}$)	Clear day with gentle winds ($s\ m^{-1}$)	Clear, hot day with light winds ($s\ m^{-1}$)
50	2.1E+01	4.4E+00	1.1E+01	3.4E+00	1.5E+00	2.1E+00	7.0E+00
100	3.9E+01	7.9E+00	1.6E+01	5.6E+00	2.5E+00	3.0E+00	9.4E+00
150	5.3E+01	1.1E+01	1.9E+01	7.2E+00	3.2E+00	3.5E+00	1.1E+01
200	6.6E+01	1.3E+01	2.1E+01	8.4E+00	3.8E+00	3.9E+00	1.2E+01
250	7.6E+01	1.5E+01	2.3E+01	9.3E+00	4.2E+00	4.2E+00	1.2E+01
300	8.6E+01	1.7E+01	2.4E+01	1.0E+01	4.6E+00	4.4E+00	1.3E+01
350	9.4E+01	1.9E+01	2.5E+01	1.1E+01	4.9E+00	4.6E+00	1.3E+01
400	1.0E+02	2.0E+01	2.6E+01	1.1E+01	5.2E+00	4.8E+00	1.4E+01
450	1.1E+02	2.1E+01	2.7E+01	1.2E+01	5.5E+00	4.9E+00	1.4E+01
500	1.1E+02	2.2E+01	2.8E+01	1.3E+01	5.7E+00	5.0E+00	1.4E+01
550	1.2E+02	2.3E+01	2.9E+01	1.3E+01	5.9E+00	5.1E+00	1.4E+01
600	1.2E+02	2.4E+01	2.9E+01	1.3E+01	6.1E+00	5.2E+00	1.5E+01
650	1.3E+02	2.5E+01	3.0E+01	1.4E+01	6.3E+00	5.3E+00	1.5E+01
700	1.3E+02	2.6E+01	3.0E+01	1.4E+01	6.5E+00	5.4E+00	1.5E+01
750	1.4E+02	2.7E+01	3.1E+01	1.4E+01	6.6E+00	5.5E+00	1.5E+01
800	1.4E+02	2.8E+01	3.1E+01	1.5E+01	6.8E+00	5.5E+00	1.5E+01
850	1.4E+02	2.8E+01	3.1E+01	1.5E+01	6.9E+00	5.6E+00	1.5E+01
900	1.5E+02	2.9E+01	3.2E+01	1.5E+01	7.0E+00	5.7E+00	1.5E+01
950	1.5E+02	3.0E+01	3.2E+01	1.6E+01	7.2E+00	5.7E+00	1.6E+01
1,000	1.5E+02	3.0E+01	3.2E+01	1.6E+01	7.3E+00	5.8E+00	1.6E+01
1,050	1.5E+02	3.1E+01	3.2E+01	1.6E+01	7.4E+00	5.8E+00	1.6E+01
1,100	1.5E+02	3.1E+01	3.3E+01	1.6E+01	7.5E+00	5.9E+00	1.6E+01
2,000	1.8E+02	3.6E+01	3.3E+01	1.7E+01	7.9E+00	6.6E+00	1.7E+01
3,000	1.9E+02	3.9E+01	3.4E+01	1.8E+01	8.5E+00	6.9E+00	1.8E+01
4,000	1.9E+02	4.2E+01	3.5E+01	1.9E+01	8.9E+00	7.1E+00	1.8E+01
5,000	2.0E+02	4.4E+01	3.5E+01	2.0E+01	9.3E+00	7.3E+00	1.8E+01
6,000	2.0E+02	4.6E+01	3.5E+01	2.0E+01	9.6E+00	7.4E+00	1.8E+01
7,000	2.0E+02	4.7E+01	3.6E+01	2.1E+01	9.8E+00	7.5E+00	1.8E+01
8,000	2.0E+02	4.8E+01	3.6E+01	2.1E+01	1.0E+01	7.6E+00	1.9E+01
9,000	2.0E+02	4.9E+01	3.6E+01	2.1E+01	1.0E+01	7.7E+00	1.9E+01
10,000	2.0E+02	5.0E+01	3.6E+01	2.1E+01	1.0E+01	7.8E+00	1.9E+01
11,000	2.0E+02	5.1E+01	3.6E+01	2.2E+01	1.1E+01	7.8E+00	1.9E+01
12,000	2.0E+02	5.2E+01	3.6E+01	2.2E+01	1.1E+01	7.9E+00	1.9E+01
13,000	2.0E+02	5.2E+01	3.6E+01	2.2E+01	1.1E+01	8.0E+00	1.9E+01
14,000	2.0E+02	5.3E+01	3.6E+01	2.2E+01	1.1E+01	8.0E+00	1.9E+01
15,000	2.0E+02	5.4E+01	3.6E+01	2.2E+01	1.1E+01	8.1E+00	1.9E+01
16,000	2.0E+02	5.4E+01	3.6E+01	2.3E+01	1.1E+01	8.1E+00	1.9E+01
17,000	2.0E+02	5.5E+01	3.6E+01	2.3E+01	1.1E+01	8.2E+00	1.9E+01
18,000	2.0E+02	5.5E+01	3.6E+01	2.3E+01	1.2E+01	8.2E+00	1.9E+01
19,000	2.0E+02	5.5E+01	3.6E+01	2.3E+01	1.2E+01	8.3E+00	1.9E+01
20,000	2.0E+02	5.6E+01	3.6E+01	2.3E+01	1.2E+01	8.3E+00	1.9E+01

Table B4b. Normalized Time and Space Integrated Particle Air Concentration for a Circle Arc at the specified distance from the release assuming airborne loss rate (λ_{decay} = 1 h^{-1}).

Distance Downwind (m)	Clear, cold night with light winds ($s\ m^{-2}$)	Clear night with gentle breeze ($s\ m^{-2}$)	Overcast with light winds ($s\ m^{-2}$)	Overcast with gentle winds ($s\ m^{-2}$)	Overcast with strong winds ($s\ m^{-2}$)	Clear day with gentle winds ($s\ m^{-2}$)	Clear, hot day with light winds ($s\ m^{-2}$)
50	3.8E-01	8.0E-02	1.3E-01	5.4E-02	2.4E-02	2.4E-02	6.8E-02
100	3.2E-01	6.3E-02	7.8E-02	3.6E-02	1.6E-02	1.3E-02	3.4E-02
150	2.7E-01	5.2E-02	5.3E-02	2.7E-02	1.2E-02	8.8E-03	2.2E-02
200	2.3E-01	4.3E-02	3.9E-02	2.1E-02	9.8E-03	6.4E-03	1.5E-02
250	2.0E-01	3.8E-02	3.1E-02	1.8E-02	8.2E-03	5.0E-03	1.2E-02
300	1.8E-01	3.3E-02	2.5E-02	1.5E-02	7.0E-03	4.1E-03	9.4E-03
350	1.6E-01	2.9E-02	2.1E-02	1.3E-02	6.1E-03	3.4E-03	7.6E-03
400	1.4E-01	2.7E-02	1.8E-02	1.2E-02	5.4E-03	3.0E-03	6.4E-03
450	1.2E-01	2.4E-02	1.5E-02	1.0E-02	4.9E-03	2.6E-03	5.5E-03
500	1.1E-01	2.2E-02	1.3E-02	9.4E-03	4.4E-03	2.3E-03	4.8E-03
550	1.0E-01	2.0E-02	1.2E-02	8.6E-03	4.0E-03	2.0E-03	4.2E-03
600	9.3E-02	1.9E-02	1.1E-02	7.9E-03	3.7E-03	1.8E-03	3.7E-03
650	8.5E-02	1.8E-02	9.5E-03	7.3E-03	3.5E-03	1.7E-03	3.3E-03
700	7.8E-02	1.6E-02	8.6E-03	6.9E-03	3.2E-03	1.5E-03	3.0E-03
750	7.2E-02	1.5E-02	7.8E-03	6.4E-03	3.0E-03	1.4E-03	2.7E-03
800	6.5E-02	1.4E-02	7.1E-03	6.0E-03	2.9E-03	1.3E-03	2.5E-03
850	6.0E-02	1.4E-02	6.5E-03	5.6E-03	2.7E-03	1.2E-03	2.3E-03
900	5.5E-02	1.3E-02	6.0E-03	5.4E-03	2.6E-03	1.1E-03	2.1E-03
950	5.0E-02	1.2E-02	5.5E-03	5.1E-03	2.4E-03	1.0E-03	2.0E-03
1,000	4.6E-02	1.2E-02	5.0E-03	4.8E-03	2.3E-03	9.7E-04	1.8E-03
1,050	4.1E-02	1.1E-02	4.6E-03	4.6E-03	2.2E-03	9.1E-04	1.7E-03
1,100	3.6E-02	1.1E-02	4.1E-03	4.3E-03	2.1E-03	8.4E-04	1.5E-03
2,000	1.7E-02	4.7E-03	1.5E-03	1.4E-03	7.2E-04	4.0E-04	6.4E-04
3,000	7.5E-03	3.1E-03	8.0E-04	9.5E-04	4.9E-04	2.5E-04	3.5E-04
4,000	3.9E-03	2.3E-03	4.9E-04	6.9E-04	3.8E-04	1.8E-04	2.2E-04
5,000	2.3E-03	1.9E-03	3.3E-04	5.5E-04	3.1E-04	1.5E-04	1.6E-04
6,000	1.4E-03	1.5E-03	2.3E-04	4.5E-04	2.7E-04	1.2E-04	1.1E-04
7,000	9.3E-04	1.3E-03	1.7E-04	3.8E-04	2.3E-04	1.1E-04	8.4E-05
8,000	6.4E-04	1.1E-03	1.3E-04	3.2E-04	2.1E-04	9.1E-05	6.6E-05
9,000	4.5E-04	9.7E-04	1.0E-04	2.9E-04	1.9E-04	8.4E-05	5.0E-05
10,000	3.2E-04	8.6E-04	7.4E-05	2.5E-04	1.8E-04	7.7E-05	3.8E-05
11,000	2.3E-04	7.7E-04	5.9E-05	2.3E-04	1.7E-04	7.2E-05	2.9E-05
12,000	1.7E-04	6.9E-04	4.7E-05	2.1E-04	1.6E-04	6.5E-05	2.3E-05
13,000	1.3E-04	6.3E-04	3.6E-05	1.9E-04	1.5E-04	6.0E-05	1.9E-05
14,000	9.7E-05	5.8E-04	2.8E-05	1.7E-04	1.4E-04	5.6E-05	1.4E-05
15,000	7.4E-05	5.3E-04	2.2E-05	1.5E-04	1.3E-04	5.1E-05	1.1E-05
16,000	5.7E-05	4.8E-04	1.7E-05	1.4E-04	1.2E-04	4.8E-05	9.2E-06
17,000	4.4E-05	4.5E-04	1.4E-05	1.3E-04	1.2E-04	4.7E-05	7.3E-06
18,000	3.4E-05	4.2E-04	1.1E-05	1.2E-04	1.1E-04	4.2E-05	5.8E-06
19,000	2.7E-05	3.8E-04	8.7E-06	1.1E-04	1.1E-04	4.2E-05	4.6E-06
20,000	2.1E-05	3.6E-04	6.9E-06	1.0E-04	1.0E-04	3.8E-05	3.8E-06

Table B5a. Normalized Time and Space Integrated Particle Air Concentration for a Disc with the specified distance from the release assuming airborne loss rate (λ_{decay} = 10 h^{-1}).

Distance Downwind (m)	Clear, cold night with light winds ($s\ m^{-1}$)	Clear night with gentle breeze ($s\ m^{-1}$)	Overcast with light winds ($s\ m^{-1}$)	Overcast with gentle winds ($s\ m^{-1}$)	Overcast with strong winds ($s\ m^{-1}$)	Clear day with gentle winds ($s\ m^{-1}$)	Clear, hot day with light winds ($s\ m^{-1}$)
50	1.7E+01	4.3E+00	9.7E+00	3.3E+00	1.5E+00	2.1E+00	6.5E+00
100	2.8E+01	7.5E+00	1.4E+01	5.4E+00	2.5E+00	2.9E+00	8.5E+00
150	3.6E+01	1.0E+01	1.6E+01	6.8E+00	3.2E+00	3.4E+00	9.4E+00
200	4.1E+01	1.2E+01	1.7E+01	7.8E+00	3.7E+00	3.7E+00	1.0E+01
250	4.4E+01	1.4E+01	1.8E+01	8.6E+00	4.1E+00	4.0E+00	1.0E+01
300	4.7E+01	1.5E+01	1.8E+01	9.2E+00	4.4E+00	4.2E+00	1.1E+01
350	4.9E+01	1.6E+01	1.9E+01	9.8E+00	4.7E+00	4.3E+00	1.1E+01
400	5.1E+01	1.7E+01	1.9E+01	1.0E+01	5.0E+00	4.4E+00	1.1E+01
450	5.2E+01	1.8E+01	2.0E+01	1.1E+01	5.2E+00	4.6E+00	1.1E+01
500	5.3E+01	1.8E+01	2.0E+01	1.1E+01	5.4E+00	4.6E+00	1.1E+01
550	5.3E+01	1.9E+01	2.0E+01	1.1E+01	5.5E+00	4.7E+00	1.1E+01
600	5.4E+01	2.0E+01	2.0E+01	1.2E+01	5.7E+00	4.8E+00	1.1E+01
650	5.4E+01	2.0E+01	2.0E+01	1.2E+01	5.8E+00	4.8E+00	1.1E+01
700	5.5E+01	2.1E+01	2.0E+01	1.2E+01	6.0E+00	4.9E+00	1.1E+01
750	5.5E+01	2.1E+01	2.0E+01	1.2E+01	6.1E+00	4.9E+00	1.1E+01
800	5.5E+01	2.1E+01	2.0E+01	1.2E+01	6.2E+00	5.0E+00	1.1E+01
850	5.5E+01	2.2E+01	2.0E+01	1.3E+01	6.3E+00	5.0E+00	1.1E+01
900	5.5E+01	2.2E+01	2.0E+01	1.3E+01	6.4E+00	5.1E+00	1.1E+01
950	5.5E+01	2.2E+01	2.0E+01	1.3E+01	6.5E+00	5.1E+00	1.1E+01
1,000	5.5E+01	2.3E+01	2.0E+01	1.3E+01	6.6E+00	5.1E+00	1.1E+01
1,050	5.6E+01	2.3E+01	2.0E+01	1.3E+01	6.7E+00	5.2E+00	1.1E+01
1,100	5.6E+01	2.3E+01	2.1E+01	1.3E+01	6.8E+00	5.2E+00	1.1E+01
2,000	6.1E+01	2.5E+01	2.1E+01	1.3E+01	7.0E+00	5.6E+00	1.2E+01
3,000	6.1E+01	2.5E+01	2.1E+01	1.4E+01	7.3E+00	5.7E+00	1.2E+01
4,000	6.1E+01	2.6E+01	2.1E+01	1.4E+01	7.4E+00	5.7E+00	1.2E+01
5,000	6.1E+01	2.6E+01	2.1E+01	1.4E+01	7.6E+00	5.8E+00	1.2E+01
6,000	6.1E+01	2.6E+01	2.1E+01	1.4E+01	7.6E+00	5.8E+00	1.2E+01
7,000	6.1E+01	2.6E+01	2.1E+01	1.4E+01	7.7E+00	5.8E+00	1.2E+01
8,000	6.1E+01	2.6E+01	2.1E+01	1.4E+01	7.7E+00	5.8E+00	1.2E+01
9,000	6.1E+01	2.6E+01	2.1E+01	1.4E+01	7.8E+00	5.8E+00	1.2E+01
10,000	6.1E+01	2.6E+01	2.1E+01	1.4E+01	7.8E+00	5.8E+00	1.2E+01
11,000	6.1E+01	2.6E+01	2.1E+01	1.4E+01	7.8E+00	5.8E+00	1.2E+01
12,000	6.1E+01	2.6E+01	2.1E+01	1.4E+01	7.8E+00	5.8E+00	1.2E+01
13,000	6.1E+01	2.6E+01	2.1E+01	1.4E+01	7.8E+00	5.8E+00	1.2E+01
14,000	6.1E+01	2.6E+01	2.1E+01	1.4E+01	7.8E+00	5.8E+00	1.2E+01
15,000	6.1E+01	2.6E+01	2.1E+01	1.4E+01	7.8E+00	5.8E+00	1.2E+01
16,000	6.1E+01	2.6E+01	2.1E+01	1.4E+01	7.8E+00	5.8E+00	1.2E+01
17,000	6.1E+01	2.6E+01	2.1E+01	1.4E+01	7.9E+00	5.8E+00	1.2E+01
18,000	6.1E+01	2.6E+01	2.1E+01	1.4E+01	7.9E+00	5.8E+00	1.2E+01
19,000	6.1E+01	2.6E+01	2.1E+01	1.4E+01	7.9E+00	5.8E+00	1.2E+01
20,000	6.1E+01	2.6E+01	2.1E+01	1.4E+01	7.9E+00	5.8E+00	1.2E+01

Table B5b. Normalized Time and Space Integrated Particle Air Concentration for a Circle Arc at the specified distance from the release assuming airborne loss rate (λ_{decay} = 10 h^{-1}).

Distance Downwind (m)	Clear, cold night with light winds (s m^{-2})	Clear night with gentle breeze (s m^{-2})	Overcast with light winds (s m^{-2})	Overcast with gentle winds (s m^{-2})	Overcast with strong winds (s m^{-2})	Clear day with gentle winds (s m^{-2})	Clear, hot day with light winds (s m^{-2})
50	2.7E-01	7.5E-02	1.1E-01	5.1E-02	2.4E-02	2.3E-02	5.7E-02
100	1.8E-01	5.6E-02	5.5E-02	3.3E-02	1.6E-02	1.2E-02	2.5E-02
150	1.2E-01	4.4E-02	3.3E-02	2.4E-02	1.2E-02	7.9E-03	1.4E-02
200	8.6E-02	3.5E-02	2.1E-02	1.8E-02	9.0E-03	5.6E-03	9.0E-03
250	6.3E-02	2.9E-02	1.5E-02	1.4E-02	7.4E-03	4.2E-03	6.2E-03
300	4.6E-02	2.4E-02	1.1E-02	1.2E-02	6.2E-03	3.4E-03	4.4E-03
350	3.4E-02	2.1E-02	7.9E-03	9.8E-03	5.3E-03	2.8E-03	3.2E-03
400	2.6E-02	1.8E-02	6.0E-03	8.4E-03	4.7E-03	2.3E-03	2.4E-03
450	2.0E-02	1.6E-02	4.6E-03	7.3E-03	4.1E-03	2.0E-03	1.9E-03
500	1.5E-02	1.4E-02	3.6E-03	6.4E-03	3.7E-03	1.7E-03	1.5E-03
550	1.2E-02	1.2E-02	2.9E-03	5.6E-03	3.3E-03	1.5E-03	1.2E-03
600	9.3E-03	1.1E-02	2.3E-03	5.0E-03	3.0E-03	1.3E-03	9.4E-04
650	7.3E-03	9.6E-03	1.9E-03	4.5E-03	2.8E-03	1.1E-03	7.5E-04
700	5.7E-03	8.6E-03	1.5E-03	4.1E-03	2.5E-03	1.0E-03	6.1E-04
750	4.6E-03	7.8E-03	1.3E-03	3.7E-03	2.4E-03	9.0E-04	5.1E-04
800	3.6E-03	7.0E-03	1.0E-03	3.4E-03	2.2E-03	8.1E-04	4.3E-04
850	2.9E-03	6.5E-03	8.6E-04	3.1E-03	2.1E-03	7.4E-04	3.6E-04
900	2.3E-03	5.9E-03	7.2E-04	2.8E-03	1.9E-03	6.7E-04	3.0E-04
950	1.8E-03	5.4E-03	6.0E-04	2.6E-03	1.8E-03	6.0E-04	2.5E-04
1,000	1.5E-03	5.0E-03	5.0E-04	2.4E-03	1.7E-03	5.6E-04	2.1E-04
1,050	1.2E-03	4.6E-03	4.2E-04	2.2E-03	1.6E-03	5.2E-04	1.8E-04
1,100	9.2E-04	4.2E-03	3.4E-04	2.0E-03	1.5E-03	4.7E-04	1.5E-04
2,000	4.9E-05	1.1E-03	2.3E-05	4.1E-04	4.0E-04	1.4E-04	1.2E-05
3,000	2.6E-06	4.1E-04	2.1E-06	1.7E-04	2.2E-04	5.5E-05	1.0E-06
4,000	2.0E-07	1.9E-04	2.5E-07	7.6E-05	1.4E-04	2.6E-05	1.1E-07
5,000	2.1E-08	9.7E-05	3.3E-08	3.9E-05	9.3E-05	1.4E-05	1.4E-08
6,000	2.2E-09	5.2E-05	4.4E-09	2.1E-05	6.6E-05	7.4E-06	1.7E-09
7,000	2.2E-10	2.9E-05	6.0E-10	1.1E-05	4.7E-05	4.2E-06	1.9E-10
8,000	1.3E-11	1.7E-05	6.4E-11	6.5E-06	3.5E-05	2.4E-06	1.7E-11
9,000	3.7E-13	1.0E-05	3.2E-12	3.8E-06	2.7E-05	1.4E-06	5.5E-13
10,000	0.0E+00	6.3E-06	9.3E-14	2.2E-06	2.0E-05	8.5E-07	0.0E+00
11,000	0.0E+00	3.9E-06	0.0E+00	1.3E-06	1.6E-05	5.3E-07	0.0E+00
12,000	0.0E+00	2.5E-06	0.0E+00	8.1E-07	1.2E-05	3.1E-07	0.0E+00
13,000	0.0E+00	1.6E-06	0.0E+00	5.0E-07	9.6E-06	1.9E-07	0.0E+00
14,000	0.0E+00	1.0E-06	0.0E+00	3.0E-07	7.6E-06	1.1E-07	0.0E+00
15,000	0.0E+00	6.8E-07	0.0E+00	1.8E-07	5.8E-06	6.8E-08	0.0E+00
16,000	0.0E+00	4.4E-07	0.0E+00	1.1E-07	4.6E-06	4.3E-08	0.0E+00
17,000	0.0E+00	3.0E-07	0.0E+00	6.9E-08	3.7E-06	2.7E-08	0.0E+00
18,000	0.0E+00	1.9E-07	0.0E+00	4.2E-08	3.0E-06	1.6E-08	0.0E+00
19,000	0.0E+00	1.3E-07	0.0E+00	2.6E-08	2.3E-06	1.0E-08	0.0E+00
20,000	0.0E+00	8.7E-08	0.0E+00	1.7E-08	1.9E-06	6.2E-09	0.0E+00

Supplemental Material S3:
Key Atmospheric Transport and Dispersion Modeling Concepts

Michael B Dillon and Ron Baskett

Atmospheric physics, as well as atmospheric transport and dispersion models of airborne hazards, are well-established fields with extensive literatures. This supplemental material aims to briefly introduce the reader to key atmospheric concepts. We note that while the theory developed in this study is applicable at a wide range of spatial and temporal scales, the epidemiological datasets that are compared to theoretical predictions here relate to exposures that occur near the earth's surface (within the atmospheric boundary layer), from 0.05 km to a few tens of km downwind of an airborne release, and with transport time scales ranging from minutes to less than a few hours from the time of initial release. The interested reader is referred to (6–13) for further details of atmospheric air flow physics, dispersion, and modeling including those present at other spatial and temporal scales.

S3.1. Mean Air Flow in the Atmosphere

The mean (time-averaged) air flows are driven by a spatial gradient in atmospheric pressure. When the horizontal surface pressure gradient between two locations is a few millibar over a hundred kilometers (tenths of mb km^{-1}), as occurs near the center of a high-pressure weather system; the atmosphere is relatively calm and horizontal surface mean wind speeds are light, typically less than 2 m s^{-1}. Larger surface pressure gradients, several to tens of mb km^{-1}, result in moderate surface winds (3 to 7 m s^{-1}) which are sufficient to stir leaves and twigs. Finally, larger pressure gradients, which can occur during storms, produce strong winds (> 8 m s^{-1}). The spatial and temporal distribution of wind, i.e., the "wind field," may be quite complex as local topography can steer the direction of local winds. For example, winds can be channeled along river and mountain valleys and within urban streets or be blocked by hills or mountains.

S3.2. Atmospheric Turbulence

In addition to the regional (mean) air flow described in the previous paragraph, smaller scale motions (turbulent eddies) are typically present in the atmosphere. These turbulent motions are due to two major causes. *Mechanically generated* turbulent motions are generated by drag resulting from the wind moving over and around physical objects on the earth's surface. The largest mechanically generated eddy size is proportional to the height above ground and obstacle size. *Buoyancy generated* turbulent motions are generated, for example, when the solar heating of the earth's surface causes warmer (buoyant) air to rise and be replaced by colder air. Buoyancy forces can also decrease turbulent motions, for example, when the surface is cooler than the air. The size of the largest buoyancy generated eddies depends on the atmospheric conditions and can be up to approximately 4,000 m.

Once generated, atmospheric eddies interact with each other and the earth's surface. These interactions result in the original eddies breaking into smaller eddies. The original eddy's (turbulent kinetic) energy is transferred to the smaller eddies. This process continues, generating successively smaller eddies until the millimeter size eddies dissipate into heat. This breakdown process results in a well-characterized spectrum of eddy sizes for a given set of atmospheric and surface conditions. One important consequence is that turbulent motions in the atmosphere are

correlated over shorter distances (and times) and become uncorrelated at larger distances (and times). Commonly, turbulent motions are correlated on timescale of a few minutes.

For many common atmospheric conditions, atmospheric eddies are at least an order of magnitude smaller (spatially and temporally) than the scales of motion present in the regional (mean) air flow. This separation provides a natural division of air motions that transport (mean winds) and dilute (turbulent eddies) contaminated air (13). This separation results in a gap in the atmospheric energy spectra associated with timescales on the order of an hour.

S3.3. Atmospheric Dispersion Physics

If a small amount of airborne material is added to a mass of air (called an air parcel), its presence will not significantly affect the regional wind, eddies, or other atmospheric properties.[5] Thus the *transport and dilution of these contaminated air parcels can be determined from atmospheric (meteorological) and surface considerations alone and does not depend on properties of the contaminant.* Furthermore, the *airborne exposure to such dilute materials can be mathematically represented as the sum of the exposure to many simpler releases* at specific locations and short time periods (superposition principle). Consequently, insights (and model results) derived for the transport and dilution of single particles released from a single location and time directly contribute to the characterization of more complex cases.

During transport by ambient winds, dispersion occurs when the turbulent eddies, described in the prior subsection, mix surrounding air with the contaminated air parcel which reduces the contamination concentration in the original air parcel and increases the contamination in neighboring air parcels. **Figure C1** shows photographs of this process using point-source smoke aerosol released at a constant rate into a constant airflow. The upper two panels are instantaneous snapshots which clearly demonstrate high moment-to-moment (stochastic) variations in plume concentrations that result from the effect of turbulent eddies. The bottom panel shows a time-lapse photograph of a smoke plume taken over several minutes. This panel shows two important turbulent dispersion regimes: First, near the release, the time-average plume crosswind spread (“width”) depends linearly on distance (and time) from the release because the turbulent motions dispersing the plume are correlated with each other. Second, and farther downwind, the plume spread becomes proportional to the square root of distance (time) from the release because the turbulent motions that disperse the contamination are no longer correlated with the motions present at the time of pollutant release to the atmosphere.

Figure C2 illustrates how the plume crosswind spread at a given downwind point increases with increasing timescales of interest (averaging time) since larger turbulent motions affect the plume spread at larger averaging times. In some cases, the growth rate of the plume width can dramatically slow after the plume outgrows the size of typical mechanically or buoyancy generated eddies. However, other processes can result in the plume width continuing to grow, for example, due to differential advection – where different parts of the plume are blown in different directions and at different speeds by variations in the mean wind. Differential advection can occur

[5] The number of particles required to change the behavior of the atmospheric depends on the (i) atmospheric volume of interest, (ii) particle size and density, (iii) release duration, and (iv) ambient wind speed (14). For context, assuming a light wind (1 m s^{-1}) and monodisperse particles as dense as water (1000 kg m^{-3}); a 1 m^3 release volume can contain at least 10^{16} 0.1 µm diameter particles, 10^{13} 1 µm diameter particles, or 10^{10} 10 µm diameter particles without violating this assumption.

under several conditions including, but not limited to, (i) variation of the mean wind with height, (ii) regional scale, horizontal, mean wind variability, and (iii) variation of the mean wind with time, e.g., diurnal wind cycles. Differential advection effects are not shown in **Figures C1** and **C2**. *We note that in the absence of additional loss mechanisms (such as radioactive decay or deposition to the earth's surface), an airborne plume will continue to transport (and dilute) far downwind – indeed plumes of airborne material have been observed on global scales.*

S3.4. Atmospheric Dispersion Models

Atmospheric transport and dispersion models simulate the previously discussed physical processes of mean wind transport and turbulent diffusion. Direct Numerical Simulation modeling, which explicitly considers all physical processes, can simulate all relevant air motions and contaminant concentrations, e.g., (15, 16). However, due to their high computational burden and extensive, and often unavailable, input data requirements, these models are not practical outside of a research environment. As such, *all practical dispersion models resolve only a portion of the atmospheric motions and physical processes while the effects of the unresolved processes are parameterized, often using statistical descriptions of turbulent motions and fits to empirical data*. As a consequence, these model results are inherently statistical in nature and, depending on the model type, predict (i) the ensemble-average (expected value) result (vast majority of models), (ii) the distribution of results (concentration fluctuation models), or (iii) a single realization from a distribution of possible flows (Computational Fluid Dynamics models using Large Eddy Simulation). Due to their ubiquity and relevance to the theory developed in this paper, we focus here on the ensemble average models. By analogy, the actual plume at any given time is one of the top two panels in **Figure C1** while the ensemble average dispersion model is predicting the time-averaged bottom panel (in steady state conditions).

There are several common types of ensemble average models, including the classic Gaussian plume model, in which downwind concentrations are calculated analytically; Gaussian puff models, in which one or more expanding "puffs" of contaminant are transported downwind; and Lagrangian particle models, in which downwind concentrations are inferred from the Monte Carlo simulations of the trajectories of computational marker particles.[6] These model types differ in their ability to resolve key spatial and temporal features as well as to describe complex scenarios. The more detailed model types typically have enhanced computational and input data requirements relative to the simpler models. All of these models will produce nearly identical results for basic scenarios and simpler flows (e.g., constant wind speed and direction) in which in the simpler models are valid (and have been validated against experimental data). Gaussian plume models are analytic solutions to transport and diffusion equations for simple conditions and are often used as part of the verification process for the more complex numerical models. *We note that the scenarios used in this study are closely related to a set of classic, straightforward scenarios and so the modeling results presented in this report are expected to be very similar to those that would be produced by different models.*

Atmospheric transport and dispersion models are generally considered to be accurate when they can reproduce individual measurements paired in time and space to within a factor of ten (or better) for a variety of different terrains, downwind distances, and environmental conditions (17,

[6] These computational marker particles are a large sample from the possible particles emitted and are used in estimating downwind concentrations along the prescribed contaminant emission amount. These particles do NOT directly represent individual physical aerosols.

18). For example, one modeling system (which is used in this study) is the LLNL ADAPT/LODI diagnostic wind field and Lagrangian particle models (19, 20). The LLNL ADAPT/LODI models have been validated against a wide range of source terms, environmental conditions, and downwind distances (0.05 to 1,500 km) (21–24). About 50% of the model-measurement comparisons are (i) within a factor of 2 to 5 for simpler releases (source terms) and environmental conditions and (ii) within a factor of 10 for more complex conditions. Most of these validation studies use gas tracers; however one experiment used particulate matter.

When model and measurement data are compared in a way that reduces the importance of stochastic variability, model accuracy can markedly improve. One case is the Quartile-Quartile (Q-Q) plot which is used, in part, to validate operational transport and dispersion models, e.g., (21, 25). This plot compares *distributions* of measured and modeled concentration data and does not have the requirement that the model/measurement data is paired in time or space. As one example, when comparing model predictions and measurements from a single tracer study that took place in Copenhagen, 38% of the point to point comparisons are within a factor of 2 but the Q-Q plot demonstrates much better agreement, see **Figure C3** (21). Another useful metric is integration within respect to time and/or space. For the Copenhagen study, all the model predictions agreed within a factor of 2 of the observed concentrations when integrated along arcs equidistant from the release site (crosswind integrated air concentrations), see **Figure C4**.

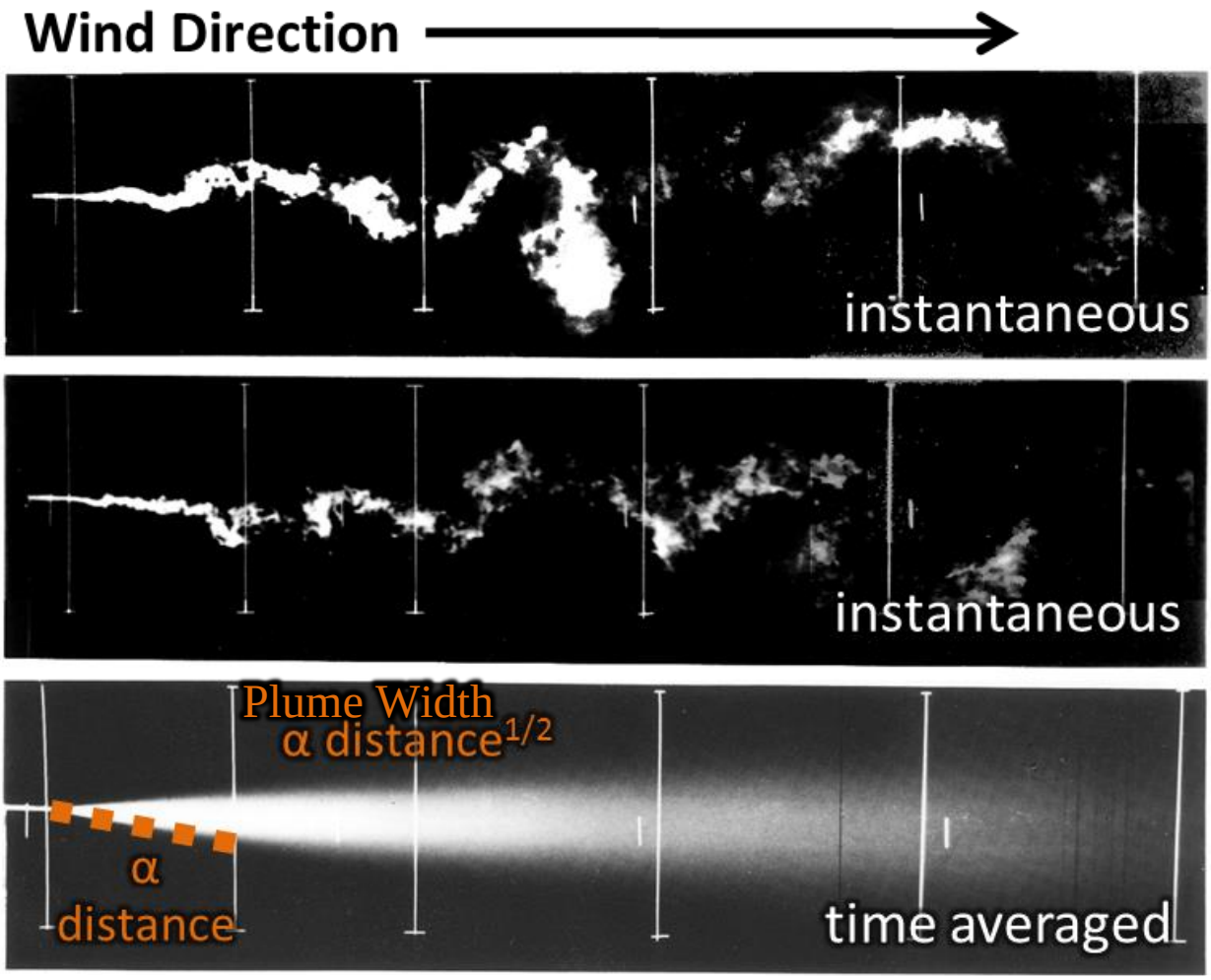

Figure C1. Laboratory photographs of plume dispersion (air flows from left to right). The top two frames are show a snapshot of an individual plume at two different times which highlight the effects of the individual eddies. The bottom frame shows a time averaged concentration over several minutes and more clearly highlight the changes in the growth rate of the plume width with time and downwind distance. (Adapted from image provided by Snyder, EPA)

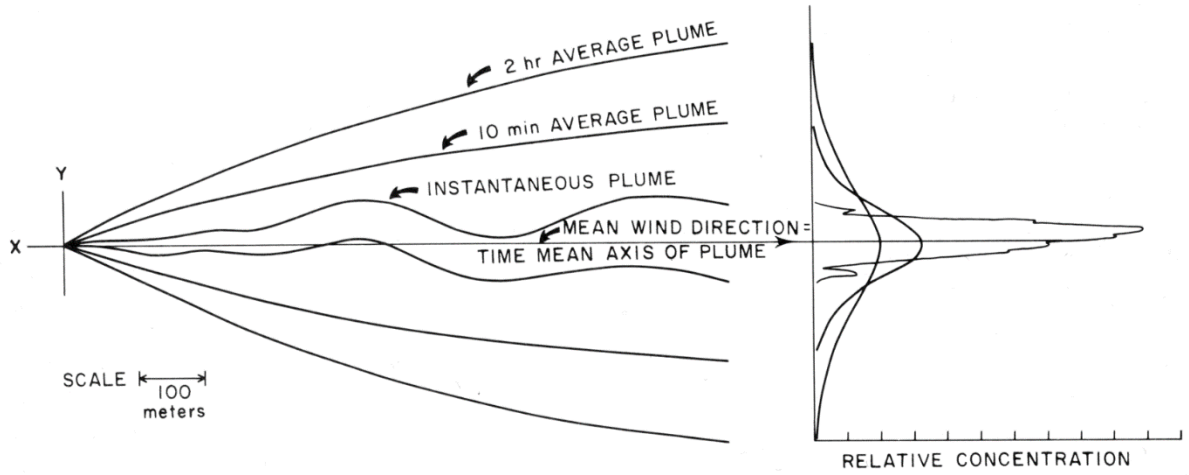

Figure C2. Illustration of the increase in plume width at a given downwind distance with averaging time taken from Slade (26). The left panel shows the nominal plume outline for one of three exemplar averaging times (wind blows along the x-axis). The right panel shows the crosswind (y axis) relative plume concentration at a single, nominal downwind point for the three averaging times considered.

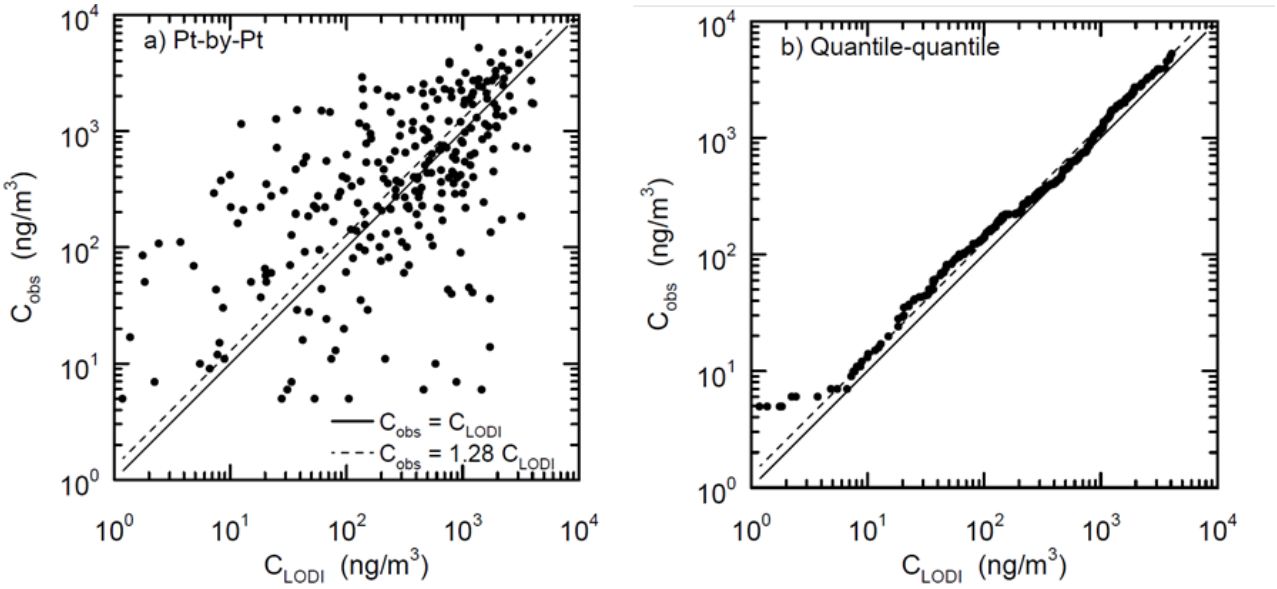

Figure C3. Observed versus predicted ground-level concentrations in the Copenhagen experiment: a) point-by-point comparison, and b) quantile-quantile comparison; only nonzero concentrations included. Dashed line corresponds to geometric mean (0.78) of LODI predicted concentration (C_{LODI}) to Observed Concentrations (C_{obs}). Image adapted from (21).

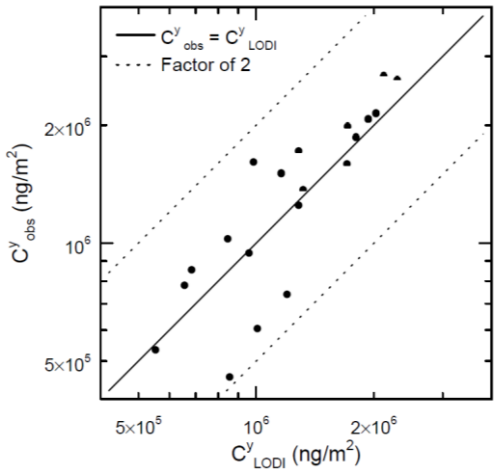

Figure C4. Comparison between observed (C^y_{obs}) and predicted (C^y_{LODI}) crosswind-integrated concentration at the surface for all Copenhagen experiments except day 7; dotted lines correspond to factor of 2 over- and under- prediction. Image adapted from (21).

Acknowledgements

The authors are grateful to their family for their support and enduring patience. The authors also thank John Nasstrom of the Lawrence Livermore National Laboratory for his considerable assistance and feedback.

Supplemental Material References
(note – reference numbering is different than in the main text)

1. US Environmental Protection Agency, “Exposure Factors Handbook 2011 Edition (Final)” (US Environmental Protection Agency).
2. M. B. Dillon, R. G. Sextro, W. W. Delp, “Regional Shelter Analysis - Inhalation Exposure Application (Particles)” (Lawrence Livermore National Laboratory, 2019). (https://figshare.com/articles/preprint/Regional_Shelter_Analysis_-_Inhalation_Exposure_Application_Particles_/9505418)
3. M. B. Dillon, C. F. Dillon, “Regional Shelter Analysis - Inhalation Exposure Methodology” (Lawrence Livermore National Laboratory, 2019). (https://figshare.com/articles/preprint/Regional_Shelter_Analysis_-_Inhalation_Exposure_Methodology/9505496)
4. J. M. Leone, *et al.*, “Lagrangian Operational Dispersion Integrator (LODI) User’s Guide v1.0” (Lawrence Livermore National Laboratory, 2001).
5. G. Sugiyama, S. T. Chan, A new meteorological data assimilation model for real-time emergency response in (American Meteorological Society, 1998), pp. 285–289.
6. A. De Visscher, *Air dispersion modeling: foundations and applications* (John Wiley & Sons, Inc, 2014).
7. S. R. Hanna, G. A. Briggs, R. P. Hosker, “Handbook of Atmospheric Diffusion” (US Department of Energy, 1982).
8. *Tracking and Predicting the Atmospheric Dispersion of Hazardous Material Releases: Implications for Homeland Security* (National Academies Press, 2003) https:/doi.org/10.17226/10716 (January 10, 2020).
9. D. Randerson, “Atmospheric science and power production” (1984).
10. S. P. Arya, *Air pollution meteorology and dispersion* (Oxford University Press, 1999).
11. D. B. Turner, “Workbook of Atmospheric Dispersion Estimates” (US Environmental Protection Agency, Office of Air Programs, 1970).
12. M. Z. Jacobson, *Fundamentals of atmospheric modeling*, 2nd ed (Cambridge University Press, 2005).
13. R. B. Stull, *An Introduction to Boundary Layer Meteorology* (Springer Netherlands, 1988) (January 23, 2020).
14. R. E. Britter, Atmospheric dispersion of dense gases. *Annu. Rev. Fluid Mech.* **21**, 317–344 (1989).
15. S. K. Shah, E. Bou-Zeid, Direct numerical simulations of turbulent Ekman layers with increasing static stability: modifications to the bulk structure and second-order statistics. *J. Fluid Mech.* **760**, 494–539 (2014).
16. S. M. I. Gohari, S. Sarkar, Stratified Ekman layers evolving under a finite-time stabilizing buoyancy flux. *J. Fluid Mech.* **840**, 266–290 (2018).

17. J. C. Chang, S. R. Hanna, Air quality model performance evaluation. *Meteorol. Atmospheric Phys.* **87** (2004).

18. P. Zannetti, Ed., *Air quality modeling: theories, methodologies, computational techniques, and available databases and software* (EnviroComp ; Air & Waste Management Association, 2010).

19. G. Sugiyama, *et al.*, Atmospheric Dispersion Modeling: Challenges of the Fukushima Daiichi Response. *Health Phys.* **102**, 493–508 (2012).

20. J. S. Nasstrom, G. Sugiyama, R. L. Baskett, S. C. Larsen, M. M. Bradley, The National Atmospheric Release Advisory Center modelling and decision-support system for radiological and nuclear emergency preparedness and response. *Int. J. Emerg. Manag.* **4**, 524 (2007).

21. J. C. Weil, “Evaluation of the NARAC Modeling System Final Report to the Lawrence Livermore National Laboratory” (Lawrence Livermore National Laboratory, 2005).

22. K. T. Foster, *et al.*, The use of an operational model evaluation system for model intercomparison. *Int. J. Environ. Pollut.* **14**, 77 (2000).

23. S. Warner, J. F. Heagy, N. Platt, M. B. Dillon, “Transport and Dispersion Model Predictions of Elevated Source Tracer Experiments in the Copenhagen Area: Comparisons of Hazard Prediction and Assessment Capability (HPAC) and National Atmospheric Release Advisory Center (NARAC) Emergency Response Model Predictions” (Institute of Defense Analysis, 2006).

24. J. S. Nasstrom, J. C. Pace, Evaluation of the effect of meteorological data resolution on Lagrangian particle dispersion simulations using the ETEX experiment. *Atmos. Environ.* **32**, 4187–4194 (1998).

25. S. G. Perry, *et al.*, AERMOD: A Dispersion Model for Industrial Source Applications. Part II: Model Performance against 17 Field Study Databases. *J. Appl. Meteorol.* **44**, 694–708 (2005).

26. D. H. Slade (Ed.), “Meteorology and Atomic Energy” (Air Resources Laboratories for the US Atomic Energy Commission, 1968).